Planet. Space Sci., Vol. 23, pp. 1621 to 1642. Pergamon Press, 1975. Printed in Northern Ireland

MASS SPECTROMETER MEASUREMENTS OF THE POSITIVE ION COMPOSITION IN THE *D*- AND *E*-REGIONS OF THE IONOSPHERE

P. A. ZBINDEN, M. A. HIDALGO,* P. EBERHARDT and J. GEISS
Physikalisches Institut, University of Bern, Sidlerstrasse 5, 3012 Bern, Switzerland

(*Received* 19 *May* 1975)

Abstract—On 14 December 1971, during the maximum of the Geminid Meteor Shower, the positive ion composition was measured in the *D*- and *E*-regions above Sardinia. The payload was launched at 12:11 UT, and measurements were made between 68·5 and 152 km altitude. A magnetic sector type mass spectrometer with dual collector and a liquid helium cryopump was used. The instrument covered the mass range from 11 to 73 AMU and had a resolution at the 1% level of $M/\Delta M = 60$.

In the *E*-region two distinct metal ion layers were observed, centred at 95 and 119 km, respectively. In the lower layer Fe^+ and Mg^+ were the most abundant metal ions, and in the upper layer Si^+ was dominant. Si^+ ions were conspicuously absent in the lower layer ($Si^+/Mg^+ < 2 \times 10^{-3}$). This particular behaviour of Si could be due to the inability of atomic oxygen to reduce SiO, whereas in the upper layer Si^+ions might be formed directly by the charge rearrangement reaction $SiO + O^+ \rightarrow Si^+ + O_2$. In addition, Na^+, Al^+, K^+, Ca^+, Ti^+, Cr^+, Ni^+ and Co^+ were also identified. The metal oxide ions AlO^+ and SiO^+ were detected, and probably also MgO^+ and $SiOH^+$. The concentrations of NO^+ and O_2^+ show a deep minimum at the maximum of the lower metal ion layer. A very high neutral metal density of 6×10^7 cm^{-3} would be required to explain this feature as resulting from charge transfer reactions between the molecular and metal ions. Such a high metal density is in contradiction to direct measurements and to cosmic dust influx rates. The isotopic ratios of Mg^+, Si^+, and of the major isotopes of Fe^+ and Ni^+ were measured, some of them with an accuracy of a few per cent ($^{25}Mg^+/^{24}Mg^+ = 0{\cdot}124 \pm 0{\cdot}006$; $^{26}Mg^+/^{24}Mg^+ = 0{\cdot}139 \pm 0{\cdot}008$; $^{29}Si^+/^{28}Si^+ = 0{\cdot}050 \pm 0{\cdot}004$; $^{54}Fe^+/^{56}Fe^+ = 0{\cdot}069 \pm 0{\cdot}005$; $^{57}Fe^+/^{56}Fe^+ = 0{\cdot}029 \pm 0{\cdot}004$; $^{60}Ni^+/^{58}Ni^+ = 0{\cdot}31 \pm 0{\cdot}12$). The isotopic ratios agree within the experimental errors with the corresponding terrestrial ratios, thus giving evidence that these elements have the same isotopic composition in the Geminid meteors as in the Earth's crust, in chrondrites, and in lunar material.

In the *D*-region the ions Na^+H_2O, $Na^+(H_2O)_2$, NaO^+ and $NaOH^+$ were tentatively identified. Below 95 km altitude the relative abundances of the ions 32^+, 33^+ and 34^+ deviate from the values expected for molecular oxygen isotopes. Their abundances can not be explained by the presence of S-ions only, and we conclude that HO_2^+ and $H_2O_2^+$ are present.

The ion density profiles of the major *D*-region constituents show some remarkable deviations from typical *D*-region conditions. These deviations are related to the winter anomaly in ionospheric absorption observed over Spain during the launch day, and our data represent the first ion composition measurements during such conditions. In particular, $H^+(H_2O)_2$ is the major ion only up to 77 km, and at 80 km altitude the NO^+ concentration exceeds the total water cluster ion density by almost two orders of magnitude. An increase of the mesospheric NO, O_3 and O concentrations as well as of the O/H_2O ratio could explain the observed ion profiles. The low NO^+/O_2^+ ratios of approximately unity measured in the *E*-region are in agreement with a strong downward transport of NO and/or O into the mesosphere during the launch day. A simple four-ion model was used to interpret our *D*-region data. The calculated neutral NO concentration increases from about 2×10^7 cm^{-3} at 85 km to 5×10^7 cm^{-3} at 80 km. In addition, evidence for an increased O_2^+ production rate above 83 km was found, probably due to an enhanced O_3 concentration. We conclude that our data strongly support vertical transport of minor neutral consituents as cause of the winter anomaly.

1. INTRODUCTION

Mass spectrometers for the study of the ion composition of the lower ionosphere have been widely used during the last ten years (cf. Istomin and Pokhunkov, 1963; Narcisi and Bailey, 1965; Krankowsky *et al.*, 1972a; Goldberg and Blumle, 1970). These experiments have shown the presence of a great variety of ions and the existence of abrupt changes in their concentrations. In many cases accurate isotopic composition measurements are required for the identification of the ions. The high speed of the rocket makes the study of regions with thin layers and other structures with high gradients

* On leave of absence from the University of Zaragoza, Facultad de Ciencias, Departamento de Fisica Fundamental, Zaragoza, Spain.

very difficult. Obviously a better understanding of the lower ionosphere can be obtained using instruments having an improved mass and altitude resolution. Our mass spectrometer was specially designed to fulfil these requirements.

The present paper reports the results obtained in the first launch of this instrument. The objective of the experiment was to study the ion composition of the midlatitude lower ionosphere and, in particular, the metal ion composition at the time of a meteor shower. The launch day was also a day of high ionospheric absorption. Thus, our results represent the first measurements of the ion composition in the *D*-region during a winter anomalous day.

2. INSTRUMENTATION

The instrument consists of a single focussing magnetic mass spectrometer, a cryopump working with liquid helium, a small sputter-ion pump, and the electronic circuitry. Figure 1 shows a cross section of the mass spectrometer and the cryopump. The mass spectrometer is a modification of a previously flown dual mode instrument (Balsiger *et al.*, 1971).

The ambient ions are attracted by the front electrode bias of -5 V and enter, together with the neutral gas, through a 2 mm dia. orifice into the cryopump. The cylinders and plates of the inlet optics accelerate and focus the ions on to the entrance slit (0·12 mm) of the mass separator. The neutral gas diffuses through the wire mesh cylinders and is condensed on the cold surfaces of the cryopump. Momentum separation is achieved in a 90° sector field of 4500 G. The mass spectrum between 11 and 73 AMU is scanned in 1·1 s by exponentially decreasing the acceleration voltage. The mass spectrometer has two exit slits (0·4 mm) in the focal plane, and thus two different masses are sampled simultaneously. The radii of curvature of the ion trajectories corresponding to the two slits are 48 and 52·2 mm. The mass ratio between the inner and the outer ion trajectory is 0·85. The ion detectors behind the two exit slits thus record the same mass with a time delay of approx. 100 msec (see Figs. 3 and 4). This double collector feature gives an improved altitude resolution. The 1% mass resolution of the analyzer is approx. 60. This resolution is superior by more than a factor of 2 to any other *D*-region mass spectrometer flown so far.

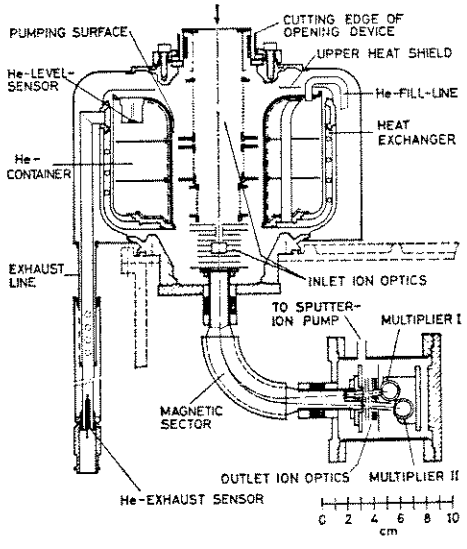

FIG. 1. CROSS SECTION OF MASS SPECTROMETER AND CRYOPUMP.

The ion current of each beam is amplified by a 10 stage electron multiplier (RCA C 70129 D) and measured by operational amplifiers (Analog Devices 301) with feedback resistors of 50 and 10 MΩ, respectively. The electrometers are followed by linear amplifiers with automatic range selectors (8 ranges, dynamic range approx. 4 decades, Baldinger and Nissen, 1967). The cryopump has a pumping speed of about 1000 ls^{-1} at internal pressures below 10^{-4} Torr. At 3×10^{-4} Torr the speed increases to 3000 ls^{-1}. Without gas load one filling of liquid helium 1·2 l. holds for 90 min. With a pressure of 1 Torr in front of the 2 mm inlet orifice the helium consumption is increased by 60%. Under laboratory conditions the pumping speed remains practically unaltered until 80–90% of the helium is evaporated. Before launch, the helium fill line is sealed, and during flight an absolute pressure valve in the exhaust line keeps the helium pressure in the reservoir at 1·1 at. A 0·4 ls^{-1} sputter-ion pump is attached to the collector region of the mass spectrometer. For high ambient gas densities this pump produces a pressure drop between cryopump and mass analyzer of approximately a factor of 10. The sputter-ion pump is also used as a pressure monitor.

The gold plated aluminium cap covering the inlet orifice is opened in flight with a device similar to the one described by Thorness and Nier (1962). This ejectable cap (not shown in Fig. 1) contains a small electron bombardment ion source which allows the residual gas spectrum to be observed for control purposes during preflight instrument checks.

The electronic circuitry and the mass spectrometer are integrated in a pressurized magnesium housing. To reduce outgassing effects the mass spectrometer is

d surfaces of the cryopump
is achieved in a 90° secto
ass spectrum between 11 an
1·1 s by exponentially decreas
oltage. The mass spectro
(0·4 mm) in the focal plane
masses are sampled simulta
rvature of the ion trajectories
vo slits are 48 and 52·2 mm
en the inner and the outer
The ion detectors behind
record the same mass with a
00 msec (see Figs. 3 and 4)
feature gives an improved
≥ 1% mass resolution of the
This resolution is superior
of 2 to any other D-region
n so far.
ach beam is amplified by a
lier (RCA C 70129 D) and
l amplifiers (Analog Devices
sistors of 50 and 10 MΩ
rometers are followed by
automatic range selectors
approx. 4 decades,
1967). The cryopump has
bout 1000 ls^{-1} at internal
orr. At 3×10^{-4} Torr the
ls^{-1}. Without gas load one
1·2 l. holds for 90 min.
r in front of the 2 mm inlet
sumption is increased by
y conditions the pumping
unaltered until 80–90% of
Before launch, the helium
during flight an absolute
aust line keeps the helium
at 1·1 at. A 0·4 ls^{-1} sputter-
the collector region of the
high ambient gas densities
essure drop between cryo-
of approximately a factor
pump is also used as a

ium cap covering the inlet
with a device similar to the
ss and Nier (1962). This
in Fig. 1) contains a small
n source which allows the
be observed for control
instrument checks.
and the mass spectrometer
riz magnesium housing.
ts the mass spectrometer is

ounted on a gas tight bulkhead. The payload
as flushed with dry nitrogen for several hours
efore launch to minimize condensation of water
apour on cold parts. The front electrode and the
et ion optics were gold plated whereas the cryo-
mp housing is polished stainless steel.

3. LABORATORY CALIBRATIONS

The effective transmission and mass discrimination
ere determined in a laboratory test chamber
Dinden, 1971). An electron bombardment source
symmetric design produces two identical, opposite
n beams of low energy (approx. 2 eV). The ion
eams have a diameter of several centimeters. The
n current is monitored with a planar Langmuir
robe mounted symmetrically to the spectrometer.
alibrations were made with Ne, N_2, Ar and Kr at
st chamber pressures ranging from 10^{-5} to 0·5 Torr.
o simulate the expected ion densities during
ight, ion currents covering a range of 3 decades
ere used. The focussing properties of the inlet
n optics depend somewhat on the external pressure.
ifferent voltage settings would be required to give
ptimal sensitivity at low and high ambient pressure.
he ion optics was adjusted to give somewhat
etter performance at lower than at higher altitudes.
he two collectors were set at different sensitivities
ensitivity ratio approx. 4) to increase the dynamic
nge to 10^5. The detection limit obtained during

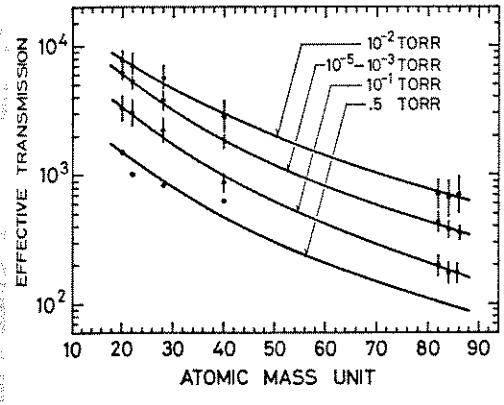

FIG. 2. EFFECTIVE TRANSMISSION OF THE COLLECTOR SYSTEM I FOR DIFFERENT TEST-CHAMBER PRESSURES.
The effective transmission is defined as the ratio between
he multiplier current and the saturation current to the
eference Langmuir electrode, normalized to the surface
f the inlet orifice. Thus, the effective transmission in-
ludes the gain of the multiplier which is also mass
ependent and in our case of the order of 10^5. The
alues are averaged over 3 current decades, and the bars
ndicate the standard errors (for the lowest curve, only
one current was measured).

flight depends on altitude and ion mass. At 110 km it varied from 2 ions cm^{-3} to 30 ions cm^{-3} from the lower to the upper end of the mass scale.

Figure 2 shows the effective transmissions measured in the laboratory. For the evaluation of the flight data the transmission was approximated by an analytical expression of the form

$$T = Am^{-\alpha}e^{-\beta m}, \qquad (1)$$

where T is the transmission, m the mass to charge ratio and A, α and β three pressure dependent parameters.

4. PAYLOAD COMPOSITION AND FLIGHT PERFORMANCE

The mass spectrometer was part of the ESRO payload S-82. The other experiments in this payload were a set of microphone detectors to measure the micrometeorite particle flux (Lindblad *et al.*, 1972), a double probe electric field detector giving ionospheric density and temperature (Pedersen *et al.*, 1972), and an ejectable parachute package with a blunt ion density probe for a total ion density measurement in the D-region (Berkeljon *et al.*, 1970). The payload was launched by a boosted Skylark rocket on 14 December 1971, near the maximum of the Geminid meteor shower and during the occurrence of a sporadic E-layer. The main flight parameters are given in Table 1.

The spectrometer entrance was opened at an altitude of 67·6 km. The current of the sputter-ion pump showed that the pressure in the mass analyzer

TABLE 1. LAUNCH CONDITIONS AND FLIGHT PARAMETERS OF ESRO PAYLOAD S-82

Range	Salto di Quirra, Sardinia
Geographic coordinates	39°36' N, 9°26' E
Date of launch	December 14, 1971
Time of launch	12.11 UT
Solar zenith angle	64°
K_p index	1^+
$F_{10.7}$	122×10^{-22} W m^{-2} Hz^{-1}
Solar X-ray (1-8 Å) flux	5×10^{-4} erg cm^{-2} s^{-1}
Apogee	152 km
Trajectory azimuth	82° (measured from north to east)
Impact ground range	177 km
Spin frequency	1.8 rps
Precession frequency	1.15 rpm
Half angle of precession cone	4.9°

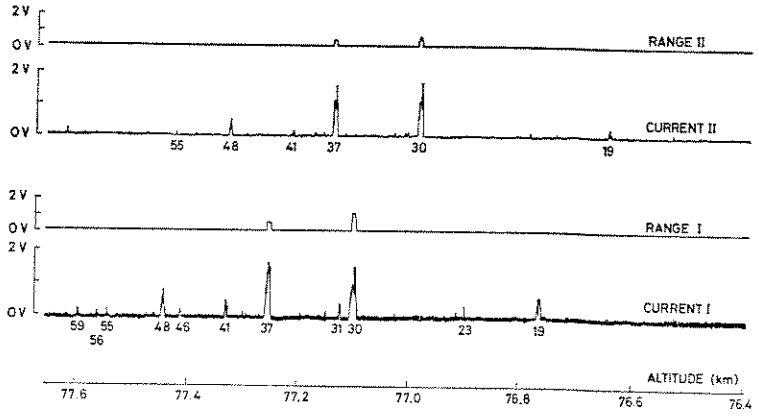

FIG. 3. MASS SPECTRUM RECORDED IN THE *D*-REGION.
The traces labelled current I and current II are the ion currents measured by the two ion detector systems. The sensitivity of the ion current amplifiers is monitored by the traces range I and range II. Each step of approx. 250 mV of the range indicator corresponds to a factor 2·5 change in the gain of the ion current amplifier. In order to increase the dynamic range channel I was made approximately a factor 4 more sensitive than channel II.

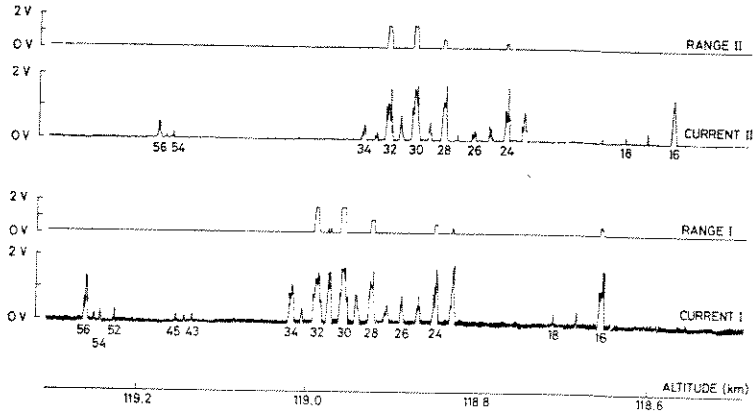

FIG. 4. MASS SPECTRUM RECORDED IN THE *E*-REGION.
For details see caption of Fig. 3.

remained below 10^{-5} Torr from the opening to a downleg altitude of 40 km. The first ion recorded was 19^+ at 68·5 km (between 67·6 and 68·5 km the mass spectrometer was scanning mass regions devoid of any ions). On the downleg, flipover occurred at 75 km. The rocket was very unstable afterwards, and only limited information on the attitude is available for this part of the flight. Ions were detected down to 61 km.

Typical examples of mass spectra recorded during the flight are shown in Figs. 3 and 4.

5. DATA REDUCTION

To determine the ion density from the recorded flight data, the measured ion currents must be corrected for the variable effective transmission (see Fig. 2). This transmission depends on the mass number and also on the pressure. In the lower part of the investigated altitude region a shock wave forms, and the ambient gas is compressed in front of the spectrometer. Thus the question arises, what pressure should be used for choosing the effective transmission.

To solve the problem for the continuum flow regime, flow patterns and gas fluxes through the inlet orifice for different flight altitudes and for laboratory conditions were numerically computed (Zbinden, 1971). An iteration method adapted from Bohachevsky and Rubin (1966) was used. The terms for heat conduction and for the ordinary

and bulk viscosity were included in order to extend the validity of the hydrodynamical equations to flows with relatively large mean free paths (see Probstein and Kemp, 1960). The gas flux measured in the laboratory agreed within 25% with the computations. The calculations showed that the gas flux into the instrument during flight is about twice the geometric gas column swept up by the orifice, and nearly equal to the influx under laboratory conditions if the test chamber pressure is equal to the stagnation pressure. It was assumed that the spectrometer transmission is only dependent on the gas influx, and therefore the calculated stagnation pressures were used for determining the effective transmission in the continuum flow regime.

At altitudes where the mean free path is comparable to or greater than the cryopump dimensions the continuum model is no longer valid. Thus, for the region above 95 km the effective pressure determining the transmission was estimated assuming molecular flow. Although this procedure is somewhat arbitrary, it will not introduce an appreciable error as the transmission remains constant at pressures below 10^{-3} Torr (equivalent to altitudes higher than 100 km).

Preliminary ion densities were obtained by dividing the measured multiplier currents by the appropriate effective transmission and using the planar approximation (Parker and Whipple, 1970). At high Mach numbers the planar approximation gives ion currents nearly equal to the ion column swept out by the inlet orifice. This procedure, also applied by other experimenters (see, e.g. Narcisi, 1971), is known to involve several uncertainties. In the free molecular flow region the major uncertainty is due to the non-zero potential of the rocket and the front electrode. In the transition and continuum flow region the problems are still more complex because, in addition to the electric field effects, the movement of the ions is strongly influenced by the neutral gas flow.

In order to reduce all the above mentioned uncertainties the preliminary mass spectrometer ion densities were normalized to electron and ion profiles measured independently by three other experiments: the ionosonde, the double plasma density and temperature probe, and the blunt total ion density probe. Ionograms were taken from the station at Capo San Lorenzo (39°30′N, 9°38′E) in short time intervals before and after the launch. This station is approximately 20 km from the launch tower and 14 km south of the ground projection of the rocket trajectory. The ionograms were evaluated by W. Becker of the Max Planck

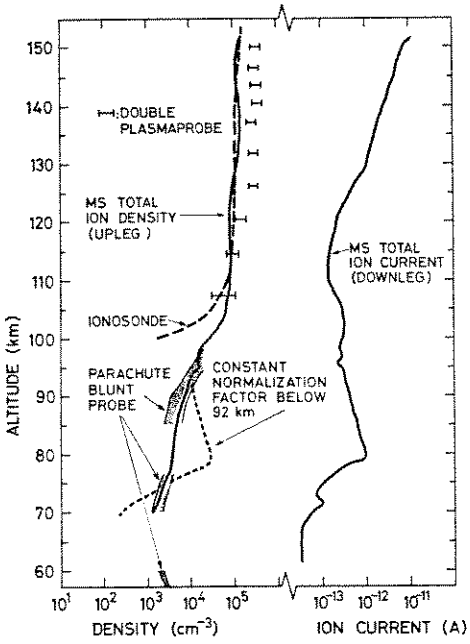

FIG. 5. TOTAL ELECTRON AND ION PROFILES.
The ionosonde profile is the average of several ionograms evaluated by Becker (1972). The double plasma probe and the parachute blunt probe were flown and evaluated by Jaeschke and Pedersen (1972). For the mass spectrometer profiles see text.

Institute for Aeronomy in Lindau, F.R.G. (Becker, 1972). The average profile obtained from several ionograms taken during the half hours immediately before and after launch is shown in Fig. 5. Also shown in Fig. 5 are the electron densities measured by the double plasma probe and the positive ion densities obtained from the parachute blunt probe (Jaeschke and Pedersen, 1972). The lower part of the double plasma probe profile agrees quite well with the ionosonde profile. At higher altitudes the double plasma probe gave systematically higher densities than the ionosonde.

The following procedure was used for adjusting the mass spectrometer data to these electron and ion profiles and to derive absolute ion densities. First, the preliminary ion densities obtained with the planar approximation were parabolically interpolated for each species to the start of every mass spectrum. Then they were summed up to give preliminary total ion density profiles for each of the two collectors. Above 110 km the ion densities were then normalized to the ionosonde profile by multiplying the preliminary ion densities with a factor smoothly varying from 0·27 at 110 km to 0·48 at apogee. The altitude dependence of the normalization factor

in this region is probably mainly due to the decrease in spectrometer transmission with increasing angle of attack. The total ion density profile of the mass spectrometer shows a wave structure at higher altitudes (see Fig. 5). This structure is anti-correlated with the angle of attack and thus is probably an artifact due to the precession modulation and not a true feature of the ionosphere. In the lower *E*-region the ionosonde profile is based on a model approximation and has probably limited physical significance (Becker, 1972). Thus, in the region from 110 to 92 km the spectrometer data were normalized to the profiles determined by Jaeschke and Pedersen (1972). This was done by smoothly increasing the normalization factor to 0·33 at 92 km.

In the *D*-region no densities are given by Jaeschke and Pedersen (1972) between 76 and 86 km. In a preliminary evaluation of our data presented at the 1973 COSPAR meeting we used a constant normalization factor of 0·33 below 92 km altitude (Zbinden *et al.*, 1974). The resulting total ion density profile obtained from the mass spectrometer data showed a considerable bulge in the 80 km region (see Fig. 5). The blunt parachute probe data gives no indication of this density bulge. As there is a gap in the data from the blunt probe, it cannot be completely excluded that a small bulge, associated with the winter anomaly present on the launch day, could exist (see also discussion of downleg data). However, the planar approximation as well as the laboratory calibrations of the mass spectrometer might not be applicable in this transition region between molecular and viscous flow.

In view of these problems we decided to normalize the spectrometer data for the final evaluation also in this region to the parachute blunt probe profile. We assumed that the ion density varies monotonically in the 76 to 86 km altitude region where no data from the parachute blunt probe are available. The resulting normalization factors are between 0·044 and 1·9. From this discussion it is obvious that the data reduction in the *D*-region includes uncertainties, and thus the true ion densities may differ from the shown profiles. Relative abundances of different ion species and isotopic ratios are not affected by these problems and are much more accurate (see discussion of isotopic and elemental abundances).

On Fig. 5 a downleg total ion profile is also plotted. As the planar approximation is unreliable at great angles of attack, only the transmission correction was made, and the curve refers to an arbitrary current scale. For the altitude region from apogee to about 77 km the rocket flew almost backwards, and the reference pressure for the transmission correction was set equal to the ambient pressure for this part of the downleg. Below this altitude the stagnation pressure was used (with a smoothed transition). The profile also shows a bulge at 80 km in spite of the different sampling conditions and transmission corrections than on the upleg.

According to the ionograms a sporadic *E*-layer with blanketing and top frequencies of 3·2 and 5 MHz, respectively, was present at approximately 110 km (Becker, 1972) whereas on the mass spectrometer ion profile no particular feature appears at this altitude (see Fig. 5). This may be explained by the fact that the sporadic *E* was only partially blanketing, and that the horizontal distance from the ionosonde to the corresponding trajectory point was about 30 km.

6. ION COMPOSITON AND STRUCTURE OF THE *E*-REGION

Figures 6 and 7 show smoothed upleg density profiles for the major ions. The following metal ions were identified: Na^{23}, Mg^{24}, Mg^{25}, Mg^{26}, Al^{27}, Si^{28}, Si^{29}, K^{39}, Ca^{40}, K^{41}, Ca^{44}, Ti^{48}, Cr^{52}, Fe^{54}, Mn^{55}, Fe^{56}, Fe^{57}, Fe^{58}, Ni^{58}, Co^{59}, Ni^{60}, Ni^{61},

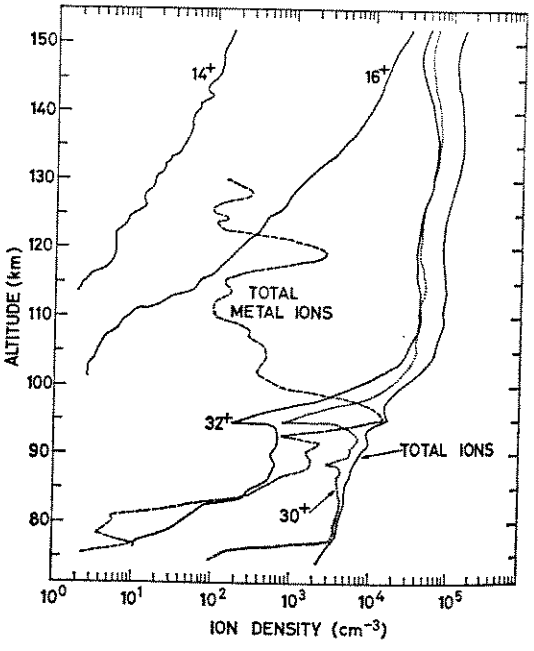

FIG. 6. UPLEG DENSITY PROFILES OF THE MAJOR POSITIVE *E*-REGION IONS.

The ions shown are N^+, O^+, O_2^+ and NO^+. The total metal ion and the total ion densities are also given. Above 122 km the total metal ion density shown must be taken as upper limit only (see Figs. 7, 10 and text).

EISS

o the ambient pressure for
. Below this altitude the
used (with a smoothed
lso shows a bulge at 80 km
sampling conditions and
han on the upleg.
grams a sporadic E-layer
frequencies of 3·2 and
present at approximately
reas on the mass spectrom-
icular feature appears at
This may be explained by
dic E was only partially
horizontal distance from
corresponding trajectory

AND STRUCTURE OF
REGION

smoothed upleg density
ns. The following metal
^{23}, Mg^{24}, Mg^{25}, Mg^{26},
^{41}, Ca^{44}, Ti^{48}, Cr^{52},
^{58}, Co^{59}, Ni^{60}, Ni^{61},

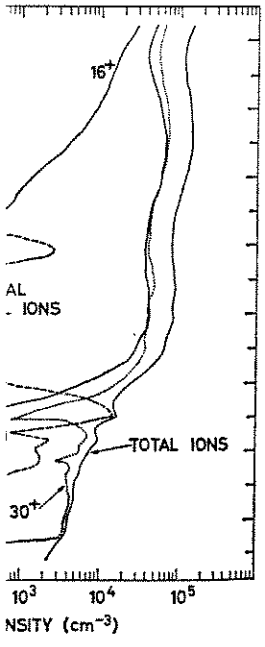

ILES OF THE MAJOR POSITIVE
N IONS.
, O_2^+ and NO^+. The total
ities are also given.
al ion density shown must
(see Figs. 7, 10 and text).

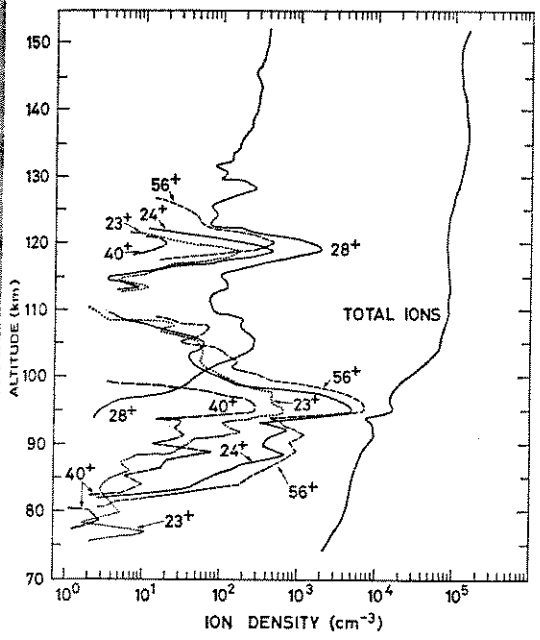

FIG. 7. UPLEG DENSITY PROFILES OF THE MAJOR METALLIC IONS DURING THE GEMINID METEOR SHOWER.
The ions shown are identified as $^{23}Na^+$, $^{24}Mg^+$, $^{28}Si^+$, $^{40}Ca^+$ and $^{56}Fe^+$ (not over whole altitude range, see text).

(Ni^{62}), (Ni^{64}), Zn^{66}. The identification of ions in parentheses is somewhat ambiguous.

At certain altitudes non metallic ions with the same mass to charge ratio as some of the above listed metals were also present. These points will be discussed in a later section.

The metal ions occur in two distinct layers with maxima at 95 and 119 km. On the downleg the ion currents measured in the lower E-region were about two orders of magnitude lower than on the upleg, and only the major metal ions were detected. They have maxima at 96 and 119 km altitude. Hence, the two major metal ion layers have horizontal extensions of at least 110 and 80 km, respectively.

In the upper layer the density maxima of the heavier metal ions are at somewhat higher altitudes than those of the lighter ones (see Fig. 7). The shift between Mg^{24+} and Fe^{56+} is approx. 1–2 km, which is more than the altitude resolution of the double collector system and thus a true ionospheric feature.

The observed metal ion profiles could be explained by the wind-shear theory of the formation of sporadic E-layers, which predicts that the layers of the long living ions follow the nodes of the gravity or tidal waves down to about 95 km and are then dumped below this altitude (see Chimonas and Axford, 1968). According to this model, the layers appear at the altitude where the ion drift velocity is approximately equal to the vertical component of the phase velocity of the wind wave. The vertical component of the ion drift velocity varies proportionally to $R_i/(1 + R_i^2)$ (see Equation 5 of Chimonas and Axford, 1968) where R_i is the ratio between the ion-neutral collision frequency and the gyrofrequency of the ions. The latter is inversely proportional to the ion mass m_i, and the former is proportional to $(r_i + r_n)^2\sqrt{(m_i + m_n)/m_i m_n}$ (m_n: mass of neutral collision partner; r_i and r_n: effective collision radius of ion and neutral, respectively, see Chapman, 1956). The R_i for Fe^{56+} is approximately a factor 2 greater than for Mg^{24+}, and we may expect that these two ions follow the node of the gravity wave with a different shift. R_i increases monotonically with decreasing altitude. At the altitude of the upper layer R_i is close to 1. For $R_i = 1$ the drift velocity has a maximum, and in first order is not mass dependent. An estimate based on a sinusoidal wind profile shows that the observed shift could be caused by a gravity wave, provided that R_i for Mg^+ was larger than 1 in the altitude region of the upper metal layer. The same mechanism could also explain the mass dependent shift of the upper edge of the lower layer and the fine structure at intermediate altitudes (107 km). Thus, the observed metal ion structure could result from a gravity wave with downward directed phase velocity transporting the recently ablated ions downwards into the broad metal ion belt, which according to Narcisi (1972) is a permanent global feature of the ionosphere.

However, the metal ion profiles might be influenced by other causes. The double plasma probe flown on the same payload measured an electric field with a component perpendicular to the rocket axis (Jaeschke and Pedersen, 1972). This field of several mV/m might produce a mass dependent shift (Kato *et al.*, 1968).

7. DISCUSSION OF THE NO^+ AND O_2^+-MINIMA

The molecular ion density shows a sharp minimum at the altitude of the lower metal ion layer (95 km, see Figs. 6 and 8). Similar profiles were observed during the Leonids and also in the absence of meteor showers (Narcisi, 1968, 1971). These minima are supposed to originate mainly from charge transfer reactions of O_2^+, NO^+, and their precursor ions with the metal atoms.

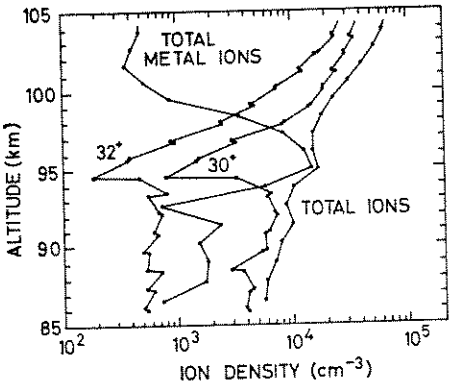

FIG. 8. FINE STRUCTURE OF THE NO^+, O_2^+, THE TOTAL METAL ION AND THE TOTAL ION DENSITY PROFILES NEAR THE MAJOR METAL ION LAYER.

For 30^+ and 32^+ all measurements from the two collectors are plotted individually. These density profiles show the good altitude resolution obtainable with our double collector mass spectrometer.

7.1 NO^+ *minimum*

Following Narcisi (1968) the NO^+ production rate q_0 in the absence of metals can be estimated by setting:

$$q_0(NO^+) = \alpha(NO^+)[NO^+]_0[e^-]_0 \qquad (2)$$

The index "o" refers to values in the absence of metals. From Fig. 8 we estimate that, if no metals were present, the following densities would exist at 94·5 km: $[NO^+]_0 = 9 \times 10^3\ cm^{-3}$; $[O_2^+]_0 = 1 \times 10^3\ cm^{-3}$; $[e^-]_0 = 1 \times 10^4\ cm^{-3}$. For a temperature of 200 K (CIRA, 1965) the recombination coefficient $\alpha(NO^+)$ is $7{\cdot}4 \times 10^{-7}\ cm^3\ s^{-1}$ (Biondi, 1969). We then obtain $q_0(NO^+) = 67\ cm^{-3}\ s^{-1}$. If the presence of metals is taken into account, a charge transfer term has to be introduced into the production-loss balance equation:

$$q(NO^+) = \alpha(NO^+)[NO^+][e^-] + k(NO^+ - M) \times [NO^+][M], \qquad (3)$$

with [M] the density of the neutral metal atoms and $k(NO^+ - M)$ the coefficient for the charge transfer from NO^+ to the metal atoms. The observed densities at 94·5 km, the altitude of the NO^+ minimum, are $[NO^+] = 8 \times 10^2\ cm^{-3}$; $[O_2^+] = 2 \times 10^2\ cm^{-3}$; $[e^-] = 1{\cdot}6 \times 10^4\ cm^{-3}$. Assuming that the production rate $q(NO^+)$ is equal to $q_0(NO^+)$, then the product $k(NO^+ - M)[M]$ becomes approximately $0{\cdot}07\ s^{-1}$, whereas Narcisi (1968) had found $0{\cdot}02\ s^{-1}$ (recalculated with the $\alpha(NO^+)$ used in the present paper).

Rutherford *et al.* (1971, 1972a, b) measured the rate coefficients for the charge transfer reactions from NO^+ to Mg, Ca and Fe at 300 K to be $8{\cdot}1 \times 10^{-10}\ cm^3\ s^{-1}$, $40 \times 10^{-10}\ cm^3\ s^{-1}$, and $9{\cdot}2 \times 10^{-10}\ cm^3\ s^{-1}$, respectively. With an average charge transfer rate of $k(NO^+ - M) = 10^{-9}\ cm^3\ s^{-1}$ a density of the neutral metal atoms of $[M] = 7 \times 10^7\ cm^{-3}$ would be required to explain the NO^+ minimum.

We have so far neglected that at 95 km a substantial fraction of the NO^+ production is due to charge transfer from O_2^+ (Ratnasiri, 1972; Danilov, 1972). In the presence of metal atoms this fraction of the NO^+ production is reduced proportionally to the ratio $[O_2^+]/[O_2^+]_0$. We may assume a neutral NO density of $4 \times 10^7\ cm^{-3}$ (Barth, 1966, see also our discussion of *D*-region results) and a charge transfer rate $k(O_2^+ - NO) = 6{\cdot}3 \times 10^{-10}\ cm^3\ s^{-1}$ (Fehsenfeld *et al.*, 1970). The NO^+ production by the charge transfer from O_2^+ is then $q_0(O_2^+ - NO) = 25\ cm^{-3}\ s^{-1}$. Hence, the NO^+ production in the presence of metals is

$$q(NO^+) = q_0(NO^+) + q_0(O_2^+ - NO)([O_2^+]/[O_2^+]_0 - 1) = 47\ cm^{-3}\ s^{-1} \qquad (4)$$

and the metal atom density

$$[M] = \frac{q(NO^+) - \alpha(NO^+)[NO^+][e^-]}{k(NO^+ - M)[NO^+]} = 5 \times 10^7\ cm^{-3}. \qquad (5)$$

According to this calculation only a small fraction of the metal atoms are ionized.

7.2 O_2^+ *minimum*

The production of O_2^+ is probably not seriously altered by the presence of metals and can be estimated from

$$q(O_2^+) = q_0(O_2^+) = [O_2^+]_0\{\alpha(O_2^+)[e^-]_0 + k(O_2^+ - NO)[NO]\} \qquad (6)$$

with $\alpha(O_2^+) = 3{\cdot}5 \times 10^{-7}\ cm^3\ s^{-1}$ at 200 K (Biondi, 1969). Using the same densities as before, $q(O_2^+) = 28\ cm^{-3}\ s^{-1}$ results. Including charge transfer to metals as an additional loss mechanism and solving the equation for the neutral metal density we obtain:

$$[M] = \frac{q(O_2^+) - [O_2^+]\{\alpha(O_2^+)[e^-] + k(O_2^+ - NO)[NO]\}}{k(O_2^+ - M)[O_2^+]}. \qquad (7)$$

The rate coefficients for the charge transfer reactions

from O_2^+ to Mg, Ca and Fe at 300 K are $1{\cdot}2 \times 10^{-9}$ $cm^3 s^{-1}$; $1{\cdot}8 \times 10^{-9} cm^3 s^{-1}$; and $1{\cdot}1 \times 10^{-9} cm^3$ s^{-1}, respectively (Rutherford *et al.*, 1971, 1972a, b). With an average charge transfer rate $k(O_2^+ - M) = 1{\cdot}5 \times 10^{-9} cm^3 s^{-1}$ a neutral metal density $[M] = 7 \times 10^7 cm^{-3}$ results from equation (7). The metal atom densities estimated from the minima in the NO^+ and O_2^+ densities agree surprisingly well.

The neutral metal atom density of approx. $6 \times 10^7 cm^{-3}$ required to explain the NO^+ and O_2^+ minima by charge transfer is hardly consistent with the measured neutral Na densities and also with the observed dust influx rates. Hake *et al.* (1972) measured the nighttime atomic Na abundance above Menlo Park (California) during the night immediately prior to the launch of our mass spectrometer. They used a tunable dye-laser. During the transit of the radiant of the Geminid meteor shower, the maximum Na density, observed at an altitude of 92 km, increased from $1{\cdot}5 \times 10^3$ cm^{-3} to $5 \times 10^3 cm^{-3}$. Assuming for the Geminid a ratio Na/total metal of 2% (Cameron, 1968), the maximum observed neutral Na density would correspond to a total neutral metal density of $2{\cdot}5 \times 10^5 cm^{-3}$. This value is more than two orders of magnitude lower than the concentration deduced from the NO^+ and O_2^+ minima.

The average width (half height) of the 95 km metal ion layer and the NO^+ and O_2^+ minima is approximately 3 km. The column density of the metal atoms required to explain the NO^+ and O_2^+ minima is thus approximately 2×10^{13} atoms cm^{-2}. The most recent estimates and measurements of the daily cosmic dust influx on the Earth are of the order of 10^4 kg d^{-1} (Hughes, 1973; Fechtig, 1974; Bibron *et al.*, 1974). Assuming chondritic composition (Urey, 1964) for the cosmic dust, this global influx rate would correspond to a daily metal atom influx of $1{\cdot}5 \times 10^{10}$ atoms $cm^{-2} d^{-1}$. A residence time of the order of 10^3 d would thus be required to explain the high neutral metal density derived from the NO^+ and O_2^+ minima.

Neither direct measurements during the Geminid shower, nor estimates from the global micrometeorite influx rates, support the high metal atom density derived from the NO^+ and O_2^+ minima. Either, the rate constants for charge transfer from molecular ions to neutral metal atoms used in our calculations are not appropriate, or other channels, e.g. involving metal oxides, are also operational.

Alternate explanations for the NO^+ and O_2^+ minima must also be considered. A thin layer (width approximately 200 m) with a peak electron density of the order of $3 \times 10^5 cm^{-3}$ moving downward with a velocity of approx. 50 ms^{-1} would lead to an NO^+ and O_2^+ minimum of the observed magnitude. However, the mass spectrometer data shows no indication of such a layer. Charge exchange on dust particles (Parthasarathy and Ray, 1966) is also five orders of magnitude too slow to explain the minimum. Thus, we have at present no satisfactory explanation for the observed NO^+ and O_2^+ structure at 95 km altitude.

8. ISOTOPIC RATIOS OF METALLIC IONS

One of the main aims of the present experiment was the measurement of the isotopic and elemental abundances of the metal ions during a meteor shower. Therefore, the rocket was launched some hours after the maximum activity of the Geminids. The Geminid meteor shower is one of the most intense showers, reaching its peak activity in the night of 13–14 December. During this time, the shower meteors are at least as frequent as sporadic meteors (Millman and MacIntosh 1964). This is supported by the 3-fold increase of neutral Na observed in the night of 13–14 December, 1971 (Hake *et al.*, 1972). A sizable fraction of the metal ions observed by our spectrometer should have originated from the Geminid shower and hence presumably represent cometary material.

The measured isotopic ratios of metallic ions are listed in Table 2. The metal ion region was divided into four altitude intervals: the region below the major metal layer, the major metal layer, the intermediate region, and the upper metal layer (see Figs. 6 and 7). The weighted averages over the four intervals are listed, too. In addition, the ratios measured by Krankowsky *et al.* (1972a) on 26 November 1969 above Andoya and the terrestrial ratios are shown.

For magnesium, silicon, iron and the main isotopes of nickel most of the measured isotopic ratios agree within the experimental error limits with the terrestrial values. Since a substantial fraction of the observed metal ions probably originated from the Geminid meteors (Hake *et al.*, 1972), we conclude that isotopic compositions in the Geminid parent comet were similar to those in ordinary chondrites and in the Earth's crust. Recently, rare phases in carbonaceous chondrites have been discovered containing O, Ne and Mg with isotopic compositions different from terrestrial material (Clayton *et al.*, 1973; Black, 1972; Eberhardt, 1974; Lee and Papanastassiou, 1974). The solar system is thus not necessarily well mixed throughout, and especially comets might contain such non equilibrated material. Our results show no variations.

TABLE 2. ISOTOPIC RATIOS OF METALLIC IONS

Isotopes	Ratios averaged over altitude intervals				Weighted average over the total altitude range a)	Ratios measured on 11, 26, 69 by Krankowsky et al. (1972 a)	Terrestrial ratios
	83 - 94 km	94 - 98 km	99 - 106 km	117 - 122 km			
Mg^{25}/Mg^{24}	0.135 ± 0.010	0.123 ± 0.007	0.117 ± 0.020	0.122 ± 0.016	0.124 ± 0.006	0.110	0.129
Mg^{26}/Mg^{24}	0.146 ± 0.007	0.137 ± 0.014	0.138 ± 0.017	0.122 ± 0.014	0.139 ± 0.008	0.111	0.142
Si^{29}/Si^{28}				0.050 ± 0.004	0.050 ± 0.004 b)		0.051
Fe^{54}/Fe^{56}	0.087 ± 0.007	0.065 ± 0.005	0.096 ± 0.053 c)	0.062 ± 0.023	0.069 ± 0.005	0.092	0.0635
Fe^{57}/Fe^{56}	0.032 ± 0.007	0.028 ± 0.004	0.043 ± 0.025		0.029 ± 0.004	0.053	0.024
Ni^{60}/Ni^{58}	0.40 ± 0.1 d)	0.24 ± 0.09 d)			0.31 ± 0.12 d)	0.27	0.39
Ni^{61}/Ni^{58}		~ 0.05 c), d)			~ 0.05 c), d)		0.02
Ni^{62}/Ni^{58}	~ 0.5 c), d)				~ 0.5 c), d)		0.054
Ni^{64}/Ni^{58}	~ 0.06 c), d)				~ 0.06 c), d)		0.016

Errors are standard deviations of the averages.

a) weighted with the reciprocal variance

b) ratio measured in 117 - 122 km layer

c) density of numerator isotope very small and measured only in 1-3 spectra of the altitude interval

d) mass 58 corrected for contribution from Fe. Identification of masses 62^+ and 64^+ as Ni isotopes is doubtful, see text.

his is not in contradiction with the observations carbonaceous chondrites, as the observed fects were small and limited to special meteorite iases.

The ratios for Ni^{62+} and Ni^{64+} are also listed in e table, but for these ions the interpretation as ickel is rather doubtful as they were only detected single spectra and did not appear in the interval the major metal layer. Also, the ratios are gher than they should be for nickel. The ion 62^+ uld possibly be identified as NO^+O_2 or Na_2O^+ d the ion 64^+ as O_4^+, SO_2^+, $Si^+(H_2O)_2$ or $O^+(H_2O_2)$.

At the maximum of the lower metal ion layer mall peaks of 41^+, 42^+ and 44^+ were detected in ddition to the larger peaks of 39^+ and 40^+. A tailed evaluation of the isotopic ratios shows that addition to Ca^+ and K^+ also MgO^+ was most kely present, with $0{\cdot}002 \leq MgO^+/Mg^+ \leq 0{\cdot}01$ see also column densities given in Table 4).

9. ABUNDANCES OF METAL- AND METAL COMPOUND-IONS

To compare the abundances of the metal-ions we alculated column densities for several altitude ntervals. This procedure was chosen because the ayer maxima of the different metals are not at the ame altitude and because silicon has a particular ertical distribution. The column densities obtained nd their abundances relative to Mg are listed in Tables 3 and 4 (Ni^{58+} was corrected in all tables for he relatively small contribution from iron). Also

TABLE 3. COLUMN DENSITY OF POSSIBLE METAL- AND METAL COMPOUND-IONS IN THE ALTITUDE INTERVAL FROM 72·3 TO 91·4 km

Mass to charge ratio	Column density ions/cm^2	Column density relative to Mg	Identification	Relative abundance of metallic element in solar system (Cameron 1968)
23	2.1×10^7	0.066	Na	0.060
24 + 25 + 26	3.2×10^8	1	Mg	1
27	2.4×10^7	0.075	Al	0.081
28	3.8×10^5	0.001	Si	0.95
39	2.2×10^7	0.069	NaO (K)	0.0029 (K)
40	2.3×10^7	0.072	Ca, (NaOH)	0.070 (Ca)
41	2.2×10^7	0.069	$Na.H_2O$	
52	1.5×10^7	0.047	Cr	0.012
54 + 56 + 57	5.4×10^8	1.69	Fe	0.85
58 + 60	3.6×10^7	0.113	Ni/NO.N_2, NO.NO)	0.044 (Ni)
59	6.9×10^6	0.022	$Na.(H_2O)_2$	0.0022 (Co)

listed in the tables are the solar system abundances given by Cameron (1968). These are mainly based on the chemical composition of carbonaceous chondrites.

9.1 *Region below major metal layer*

The ion composition in the region below the major metal layer is very complex and the identification often ambiguous (see Table 3 and Fig. 9). Traces of metallic ions (Mg^+ and Fe^+) were detected down to 73 km altitude. The measured abundances of Na^+, Al^+ and Ca^+ relative to Mg^+ agree surprisingly well with the solar system values. Fe^+ and Ni^+ are approximately a factor of two overabundant. Na^+ has a rather different altitude distribution than Mg^+, and the agreement of its abundance with the solar system value may be fortuitous. The ions 58^+ and 60^+ could also have a contribution from NO^+N_2 and NO^+NO or SiO_2^+, respectively. However, the $60^+/58^+$ ratio agrees fairly well with the isotopic abundances of Ni, and we conclude that a substantial fraction of these ions, especially in the upper part of the *D*-region, are metallic.

In the *D*-region the ions 41^+ and 59^+ are correlated with $H^+(H_2O)_2$ and NO^+H_2O (see Figs. 9 and 12). Below 90 km the $41^+/39^+$ ratio is distinctly higher than the K^{41}/K^{39} ratio. At lower altitudes 41^+ is even more abundant than 39^+. We therefore identify 41^+ as Na^+H_2O and 59^+ as $Na^+(H_2O)_2$ (41^+ has been detected and identified before by Narcisi, 1972).

The $39^+/Mg^+$ ratio is on the average approximately a factor of 20 higher than the corresponding solar system value (see Table 3). Below an altitude of 88 km the ion 39^+ is more abundant than 23^+. It seems very unlikely that this is due to a peculiar chemical behaviour of K, and we identify 39^+ in this altitude range as NaO^+. The contribution of $H^+(H_2O^{16}H_2O^{18})$ to 39^+ is less than 15% for altitudes above 76 km. Below 84 km the $40^+/Mg^+$ and $40^+/Fe^+$ ratios are larger than at higher altitudes (Fig. 7). This could be explained by the presence of $NaOH^+$. The occurrence of 40^+ in two spectra at the maximum of the Na compound ions (altitude 79 km, see Fig. 9) tends to support this identification. In the same two spectra 55^+ is also present and could either be $H^+(H_2O)_2$ or NaO_2^+ (see Figs. 9 and 12).

9.2 *Major metal layers and E-region*

The dominant metal ions are Fe^+ and Mg^+ in the lower layer and Si^+ in the upper layer (Table 4 and Fig. 7). The abundance of most metal ions relative to Mg^+ are within a factor of 2 identical with

c) ratio measured in 117 - 122 km layer
d) density of numerator isotope very small and measured only in 1-3 spectra of the altitude interval
e) mass 58 corrected for contribution from Fe. Identification of masses 62^+ and 64^+ as Ni isotopes is doubtful, see text.

TABLE 4. COLUMN DENSITIES OF METAL- AND METAL OXYDE-IONS IN THE LOWER AND UPPER METAL ION LAYER

Mass to charge ratio	Column density lower layer (93.8-98.4 km) ions/cm^2	relative to Mg	upper layer (116.7-121.9 km) ions/cm^2	relative to Mg	Identification	Relative abundance of metallic element in solar system (Cameron, 1968)
23	2.3×10^8	0.12	3.8×10^7	0.27	Na	0.060
24 + 25 26	1.9×10^9	1	1.4×10^8	1	Mg	1
27	6.8×10^7	0.036	2.7×10^6	0.019	Al	0.081
28 + 29*	3.9×10^6	0.002	5.5×10^8	3.9	Si	0.95
39	2.0×10^7	0.011	8.5×10^5	0.006	K, NaO	0.0029 (K)
40	8.7×10^7	0.046	3.4×10^6	0.024	Ca, ($Mg^{24}O$)	0.070 (Ca)
41	1.0×10^6	0.0005			K, $Mg^{25}O$	
42	1.2×10^6	0.0006			Ca, $Mg^{26}O$	
43	6.0×10^5	0.0003	1.4×10^6	0.010	AlO	
44	2.4×10^6	0.001	1.8×10^6	0.013	Ca, SiO	
45			2.6×10^6	0.019	SiOH. (Sc)	3.0×10^{-5} (Sc)
48	1.4×10^6	0.0007			Ti	0.0022
52	3.1×10^7	0.016	3.6×10^6	0.026	Cr	0.012
54 + 56 + 57	2.6×10^9	1.37	1.3×10^8	0.93	Fe	0.85
58 + 60	7.1×10^7	0.037	3.6×10^6	0.026	Ni	0.044
59	3.0×10^6	0.0016			Co	0.0022
66	2.1×10^6	0.0011			Zn	0.0014

* In the lower layer 29^+ is not Si, and the column density given for this layer is for 28^+ only.

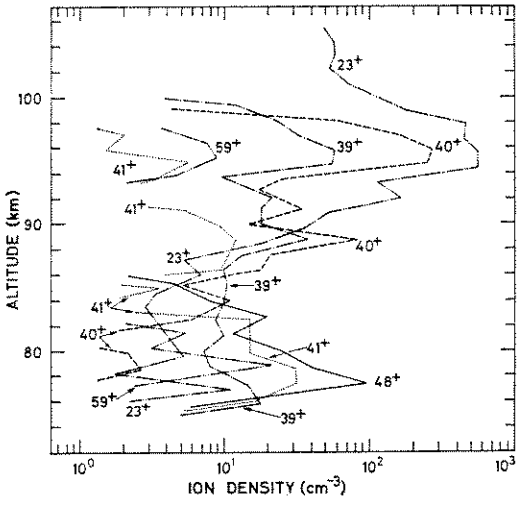

FIG. 9. UPLEG *D*-REGION PROFILES OF 23^+, 39^+, 40^+, 41^+, 48^+ AND 59^+.

Ions 23^+ and 48^+ are identified as Na^+ and NO^+H_2O respectively. In the region above approximately 90 km, 39^+ consists of a mixture of $^{39}K^+$ and NaO^+. Ions 40^+, 41^+ and 59^+ are predominantly $^{40}Ca^+$, $^{41}K^+$ and $^{59}Co^+$. In the lower region these ions are assumed to be mainly NaO^+, $NaOH^+$, Na^+H_2O and $Na^+(H_2O)_2$, respectively.

the solar system abundances. A notable exception is silicon.

The abundance profile of silicon (28^+) is distinctly different from all other metal ions (Fig. 7). In the lower layer Si^+ ions are virtually not present, and it is also absent in the *D*-region (see Table 3). This absence of Si^+ in the 90 to 100 km metal layer has also been observed in other rocket flights (Goldberg and Blumle, 1970; Narcisi, 1968). In the 119 km layer Si^+ is clearly present and the Si^+/Mg^+ ratio a factor of 4 higher than the expected solar system value. The identification of 28^+ as Si^+ in this layer is substantiated by the observed $29^+/28^+$ ratio (Table 2 and Fig. 10). The measured $29^+/28^+$ value agrees within 2% with the terrestrial Si^{29}/Si^{28} ratio.

Basically, the difference in the profiles of Si^+ and those of metallic ions (Na^+, Mg^+, Fe^+, etc.) is probably due to the fact that the oxides of the proper metals can be reduced by atomic oxygen, whereas SiO cannot (cf. Swider, 1969). Thus, silicon will be present in the upper atmosphere in the oxidized state, and consequently the ions SiO^- and SiO_2^+ will be formed primarily. Their abundances are, however, suppressed because of their short lifetimes and high ionization potentials (Swider, 1969). While these considerations easily explain

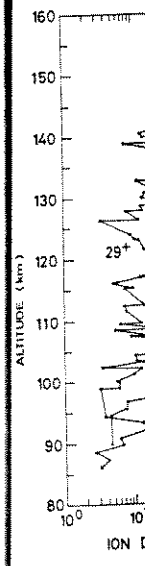

FIG. 10. DEN
In some of th
systems below
scale these p
ratios shown
averaged over

the absence
account for
layer. The
altitude of th
in forming t
charge rearr
O_2 would
rate is proba

Outside th
as Si^{28} is q
100 km the
reconciled w
(Fig. 10).
be N_2^+ and
not be inter

Above 12
quite well
concentratic
the small co
additional s
then the ion
The paralle
above 125 k
and 29^+.
reaction

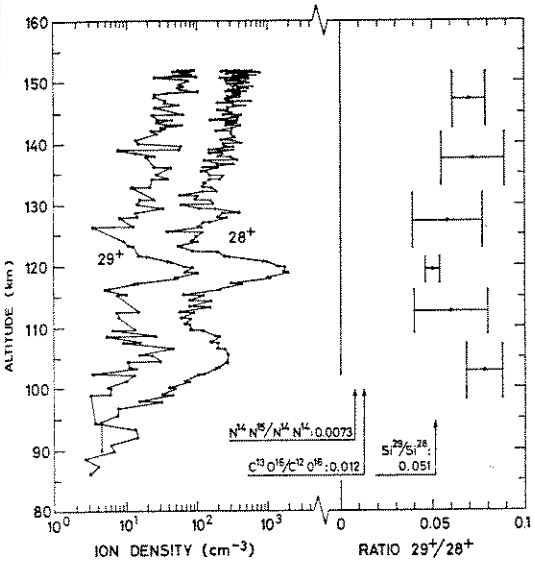

FIG. 10. DENSITIES OF 28^+ AND 29^+ AND THEIR RATIO. In some of the spectra 29^+ falls in one or both collector systems below the detection limit. Due to the logarithmic scale these points cannot be shown on the plot. The ratios shown for the different altitude intervals are averaged over all spectra including those with disappearing 29^+.

the absence of Si^+ in the lower layer, they do not account for the high abundance of Si^+ in the upper layer. The much higher abundance of O^+ at the altitude of the upper layer could perhaps play a role in forming the atomic ion of silicon. In fact, the charge rearrangement reaction $SiO + O^+ \rightarrow Si^+ + O_2$ would be exothermic, although the reaction rate is probably quite small.

Outside the upper layer the identification of 28^+ as Si^{28} is questionable. Above 132 km and below 100 km the measured $28^+/29^+$ ratio can hardly be reconciled with the terrestrial Si isotopic composition (Fig. 10). Alternate interpretations for 28^+ would be N_2^+ and CO^+. However, in this case 29^+ could not be interpreted as an isotope of the 28^+ ion.

Above 125 km the observed 28^+ densities agree quite well with the theoretically predicted N_2^+ concentrations (Hunt, 1973), except perhaps for the small concentration bulge at 128 km (possibly an additional small Si^+ layer). If 28^+ is indeed N_2^+, then the ion 29^+ must be due to a different molecule. The parallelism of the 28^+ and 29^+ profiles, even above 125 km, suggests a genetic link between 28^+ and 29^+. This link might be provided by the reaction

$$N_2^+ + H_2O \rightarrow N_2H^+ + OH \qquad (8)$$

(Shahin, 1966). In our laboratory calibrations of the spectrometer with N_2 we also observed a 29^+ peak in excess of the $N^{14}N^{15}$ contribution, even if the N_2 was dried at dry ice temperature [$p(H_2O)/p(N_2) < \sim 10^{-6}$]. This excess on mass 29^+ was substantially reduced when the N_2 was dried at liquid air temperature.

The indigenous water vapour pressure in the *E*-region is certainly too small to sustain the reaction (8) at the required high rate. However, condensation of water and the formation of ice on the cold parts of the liquid He exhaust line could not be completely avoided during the countdown, and substantial H_2O outgassing of the payload during flight has certainly occurred. Water vapour ions OH^+, H_2O^+ and H_3O^+ were indeed detected above 115 km altitude. Especially the H_2O^+ abundance was well correlated with the O^+ density ($18^+/16^+ \approx 7\%$; $17^+/16^+ \approx 1\%$), and we believe that these water vapour ions were products of charge exchange reactions between O^+ and water vapour desorbed from the payload. The $29^+/28^+$ ratio is similar to the $18^+/16^+$ ratio and according to Howard *et al.* (1970) the rate constants of reaction (8) and of the charge exchange reaction between O^+ and H_2O are nearly equal. As the recombination reactions of H_2O^+ and N_2H^+ may have rate constants of similar magnitude, this observation supports the identification of the excess 29^+ as N_2H^+ resulting from the reaction between N_2^+ and H_2O originating from the payload.

Below 100 km the ion 29^+ becomes more abundant than 28^+, forming a layerlike structure at 93 km. This could be due to atmospheric HCO^+ (Swider, 1970; Burke, 1972). The estimated contribution of N_2H^+ from the reaction $N_2^+ + H_2 \rightarrow N_2H^+ + H$ (Hierl *et al.*, 1973) is too small to be of any importance.

In the upper metal layer 45^+ was detected in a few spectra (see Fig. 4). The identification of this ion as Sc^+ seems questionable as the resulting Sc^+/Mg^+ ratio would be three orders of magnitude higher than the corresponding solar system abundance ratio. Possible other identifications are $SiOH^+$, Al^+H_2O, NH_2^+HCO and NO^+CH_3. Goldberg and Aikin (1972a) observed similarly high 45^+ abundances in the β-Taurids. Their preferred explanation is an enhancement of Sc in cometary material. We do not see any geochemical justification in this assumption. Goldberg and Aikin (1972a) observed a fairly constant $45^+/28^+$ ratio of 0·005 in their layer and at lower altitudes, which suggests a genetic relationship between 45^+ and 28^+. Also in our case the 45^+ correlates much better with

28^+ than with the major metal ions. We thus prefer to identify 45^+ as $SiOH^+$.

As discussed in a preceding section, traces of 41^+ and 42^+ were seen at the maximum of the lower metal layer giving evidence for the presence of MgO^+. Also a contribution from NaO^+ to 39^+ is most probable. In both metal layers the ions 43^+ and 44^+ were detected (see also Fig. 4). In the lower layer these ions are identified as AlO^+ and Ca^{44+}. In the upper layer ion 44^+ can not be Ca^{44+} as the $40^+/44^+$ ratio is much smaller than the Ca^{40}/Ca^{44} ratio. In this altitude range we tentatively identify 44^+ as SiO^+ and 43^+ again as AlO^+. As stated above, the observed metal ion abundances are remarkably similar to the estimated average solar system abundances of the elements (see Table 4). Any firm cosmochemical interpretation beyond this general observation would require additional knowledge on neutral-ion reactions of metals and an improved understanding of the dynamics of ion layers. Nevertheless, some of the observed systematics are suggestive, and we list them here without drawing final conclusions concerning their significance:

1. Within the limits of error ion abundances agree with solar system abundances for elements with similar chemical behaviour, e.g. Fe/Mg; Al/Ca/Ti.

2. The low abundances of the ions of S and Si in the lower layer, are probably due to fundamental differences between the ion chemistry of the metals and these elements.

3. Alkali ions are overabundant by a factor of about 2. This is probably due to their low ionization potentials and does not necessarily reflect a high abundance of these elements in the parent material.

4. There is no indication for a large metal/silicate fractionation in the parent comet.

5. The refractory elements Al, Ca, Ti (and possibly, but to a lesser extent, the less refractory Mg) are underabundant by a factor of 2–3. This could reflect a true cosmochemical abundance difference, but we cannot exclude that this observed underabundance is produced in the ionosphere.

10. IONS 32^+, 33^+ AND 34^+

Figure 11 shows the 32^+, 33^+ and 34^+ profiles and the $33^+/32^+$ and $34^+/32^+$ ratios. The high resolution of our mass spectrometer allowed for the first time the measurement of the $33^+/32^+$ ratio (cf. Fig. 4). Above 95 km the ratios agree excellently with the values expected from the isotopic composition of atmospheric O_2. At lower altitudes both ratios increase considerably. A high $34^+/32^+$ ratio in the lower mesosphere has been found previously by other investigators and has been assigned to the presence of S^+ ions (Narcisi *et al.*, 1969). A detailed analysis of our data in the 94–84 km interval reveals that the simultaneously measured $33^+/32^+$ and $34^+/32^+$ ratios can hardly be reconciled with the presence of S^+ and O_2^+ ions only. The $33^+/32^+$ reaches the S^{33}/S^{32} value at a distinctly higher altitude than the $34^+/32^+$ and S^{34}/S^{32} abundance ratio. Our data could be explained by the presence of HO_2^+ and $H_2O_2^+$ with a ratio $H_2O^+/H_2O_2^+$ of approximately unity. The existence of $H_2O_2^+$ in the *D*-region has recently been stipulated by Arnold and Krankowsky (1974). Below 82·5 km the measured $33^+/32^+$ and $34^+/32^+$ ratios do not exclude the possible presence of S^+. This could be fortuitous as indicated by the increase in both ratios below 80 km.

11. *D*-REGION RESULTS

Ion profiles of the major constituents measured during the upleg and downleg part of the rocket flight are given in Figs. 12 and 13. Because of the large angle of attack the planar approach cannot be used for the downleg data. Only a correction for the mass dependent instrument transmission was applied and the data then normalized to the total ion density profile given by Jaeschke and Pedersen (1972). The ion compositions measured in the upleg and downleg agree remarkably well.

On 14 December 1971, the transmitter–receiver link (2·83 MHz) between Aranjuez and Balerma in Spain (midpoint coordinates 38·38°N/3·24°W), operated by the Max Planck Institute for Aeronomy, Lindau, Germany, measured a high absorption with $\bar{L}_M = 48$ db (Rose *et al.*, 1973). Prior studies made with a radio link from Cape San Lorenzo (Sardinia) to Marinella (Rome) showed a cross correlation coefficient of 0·9 with the absorption measurements over Spain (Widdel, 1973). We may thus assume with great confidence that anomalous absorption conditions were also present over Sardinia during the launch day.

Prior to our experiment, the ion composition of the mesosphere during anomalous winter days was unknown. The bulk of information on this phenomenon has been obtained by ground based radio wave absorption studies (Dieminger *et al.*, 1968; Thomas, 1968). Only the total positive ion density (Hale, 1973) and the total electron concentration (Sechrist *et al.*, 1969; Mechtly *et al.*, 1973) were measured *in situ*. These experiments demonstrated that the winter anomaly is characterized by a large enhancement of the electron density in the region between 65 and 85 km. Electron concentrations 10

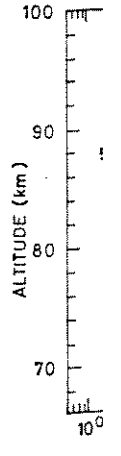

FIG. 12. U
30^+ (NO^+)
(NO_2^+); 48

ssigned to the presence
9). A detailed analysis
interval reveals that the
$33^+/32^+$ and $34^+/32^+$
ed with the presence of
e $33^+/32^+$ reaches the
igher altitude than the
ance ratio. Our data
presence of HO_2^+ and
$_2O_2^+$ of approximately
$_2^+$ in the *D*-region has
rnold and Krankowsky
measured $33^+/32^+$ and
e the possible presence
ous as indicated by the
80 km.

RESULTS

constituents measured
eg part of the rocket
nd 13. Because of the
ar roach cannot be
nly a correction for the
ansmission was applied
zed to the total ion
eschke and Pedersen
measured in the upleg
y well.
e transmitter–receiver
ranjuez and Balerma
ates 38·38°N/3·24°W),
nstitute for Aeronomy,
a high absorption with
). Prior studies made
an Lorenzo (Sardinia)
d a cross correlation
orption measurements
We may thus assume
nomalous absorption
er Sardinia during the

e ion composition of
ulous winter days was
ation on this phenom-
ground based radio
minger *et al.*, 1968;
l positive ion density
lectron concentration
ly *et al.*, 1973) were
ri s demonstrated
aracterized by a large
density in the region
on concentrations 10

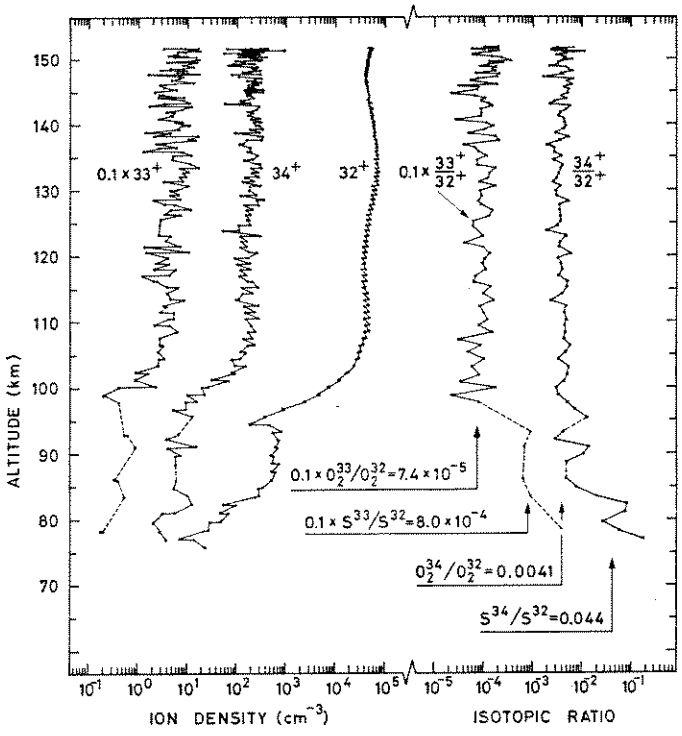

FIG. 11. DENSITIES OF 32^+, 33^+ AND 34^+ AND THEIR RATIOS.
Each point of the density plot corresponds to a value measured with one collector. Due to the logarithmic scale 33^+ and 34^+ values falling below the detection limit cannot be shown. Each point of the ratio plot corresponds to a ratio averaged over the two channels of one spectrum (including the values where 33^+ or 34^+ was below the detection limit). The dashed parts of the plot indicate spectra where 33^+ or 34^+ was in both channels below the detection limit.

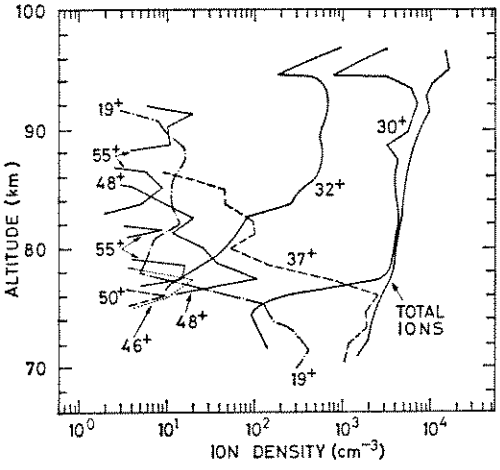

FIG. 12. UPLEG *D*-REGION PROFILES OF 19^+ (H^+H_2O); 30^+ (NO^+); 32^+ (O_2^+ or S^+); 37^+ ($H^+(H_2O)_2$); 46^+ (NO_2^+); 48^+ (NO^+H_2O); 50^+ ($O_2^+H_2O$); 55^+ ($H^+(H_2O)_3$ OR NaO_2^+).

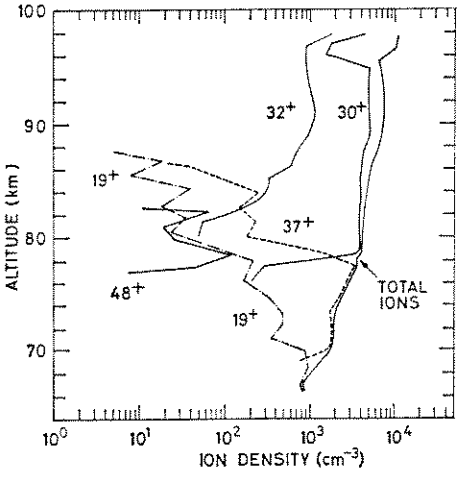

FIG. 13. DOWNLEG *D*-REGION PROFILES OF 19^+ (H^+H_2O); 30^+ (NO^+); 32^+ (O_2^+); 37^+ ($H^+(H_2O)_2$); 48^+ (NO^+H_2O).
Accuracy of altitude determinations in downleg part of flight is approx. ±1 km.

to 50 times higher than on a normal winter day were observed at an altitude of 82 km. It is evident that the high ion densities measured on 14 December reflects the presence of the anomaly over Sardinia at launch time. Our measurements show that the high electron concentration characteristic for the winter anomaly is balanced below 77 km by an increased water cluster ion density and above 77 km by an enhanced NO^+ concentration.

Our data show indeed some important departures from typical *D*-region ion profiles reflecting these anomalous conditions. Under quiescent conditions $H^+(H_2O)_2$ is dominant up to 83 km (Narcisi and Bailey, 1965). As seen in Figs. 12 and 13, we observed that water clusters are the main ions only up to 77 km. The NO^+ density increases sharply at 76 km, and NO^+ is the dominant ion above 77 km. Mass 48^+ shows a similarly high gradient. This close relationship suggests the identification of 48^+ as $NO^+(H_2O)$. The densities of both $19^+(H^+H_2O)$ and $37^+(H^+(H_2O)_2)$ decrease by a factor of 20 between 76 km and 78 km. Their concentrations remain then approximately constant until 85 km. The very good agreement of the upleg and downleg profiles, with their different measuring conditions, clearly establishes the authenticity of these features and excludes the possibility that they are artifacts produced by the sampling conditions or the data reduction.

12. THE WINTER ANOMALY

Two mechanisms might contribute to the enhancement of the winter *D*-region electron density and the associated increase in radio wave absorption (cf. Sechrist, 1972b): (a) enhancement of the precipitating particle flux; (b) changes in the minor neutral components of the atmosphere because of meteorological influences. As seen in Table 1, magnetic activity during the S-82 launch day was low ($\Sigma K_p = 5^+$). The magnetograms taken at the Ebro Observatory (Tortosa, Spain; 40°43′N; 0°30′E) showed no deviation from quiet conditions (Cardús 1974). Thus, an enhancement in the ion production due to an increase in precipitated energetic electrons as proposed by Maehlum (1967) can be excluded, at least in our case. Before the launch day, the highest disturbances observed were on 3 December with $\Sigma K_p = 20$ and on 13 December with $\Sigma K_p = 22^+$. Thus, most likely storm after-effects (composition changes at auroral latitudes and transport to middle latitudes, cf. Belrose and Thomas, 1968) were not involved in this anomalous winter day. We may then conclude that the measurements reported here correspond to an anomalous day in which energetic particle precipitation was not relevant.

In the undisturbed midlatitude daytime *D*-region, chemical processes and transport determine the electron density. Longlived minor neutral species, such as NO, O and H_2O, play a dominant role in the production or loss processes either directly or indirectly (Sechrist, 1972b; Thomas, 1971). Theoretical models predict that their altitude distribution can be modified by transport in the mesosphere and lower thermosphere (Shimazaki and Laird, 1970; Bowman *et al.*, 1970). It has been proposed that the observed winter variability in electron densities (the winter anomaly is an extreme case) could be related to changes in the mesospheric composition caused by dynamical effects. Two different processes are thought to operate: variation in turbulent mixing (Zimmerman and Narcisi, 1970; Hines, 1972) or vertical and horizontal advection on the planetary wave scale (Geisler and Dickinson, 1968; Gregory and Manson, 1969; Christie, 1970). The relative importance of these processes for the transport of minor neutral constituents during a winter anomaly is still not known. It is interesting to note that the ionograms taken during the whole launch day show the presence of gravity waves (Becker, 1972). Instabilities due to these waves may produce regions of enhanced turbulence (Hines, 1972).

The above mentioned transport mechanisms ought to affect the ion concentration not only in the *D*-, but also in the *E*-region (Bowhill, 1969). During daytime, O_2^+ and N_2^+ are the major initially formed ions in the *E*-region, and the resulting NO^+/O_2^+ ratio depends upon the O/O_2 ratio and the NO concentration. If the concentrations of these neutral constituents are modified by the transport processes operating during anomalous winter days, then this should influence the NO^+/O_2^+ ratio in the *E*-layer.

Different sets of daytime midlatitude NO^+/O_2^+ ratios are compared in Table 5. Most of the measurements were made during normal conditions. The NO^+/O_2^+ ratio is then typically between 2 and 5 (see Monro and Bowhill, 1969; Danilov, 1972). Only two measurements of the *E*-region during an anomalous winter day are available, our own and those of Narcisi (1973). Both give distinctly lower NO^+/O_2^+ ratios. Thus, the available data strongly suggest that the NO^+/O_2^+ ratio in the *E*-region is altered by the processes leading to the anomalous winter day conditions.

Our data can be compared with the theoretical calculations of Keneshea *et al.* (1970) (Fig. 14).

s day in which energetic
ot relevant.
itude daytime *D*-region,
ansport determine the
l minor neutral species,
y a dominant role in the
sses either directly or
Thomas, 1971). Theo-
heir altitude distribution
t in the mesosphere and
zaki and Laird, 1970;
has been proposed that
ity in electron densities
extreme case) could be
esospheric composition
Two different processes
variation in turbulent
Narcisi, 1970; Hines,
ontal advection on the
r and Dickinson, 1968;
969; Christie, 1970).
these processes for the
constituents during a
own. It is interesting to
ke during the whole
ence of gravity waves
due to these waves may
ed turbulence (Hines,

ransport mechanisms
ıtration not only in the
Bowhill, 1969). During
major initially formed
he resulting NO^+/O_2^+
O_2 ratio and the NO
centrations of these
lified by the transport
nomalous winter days,
NO^+/O_2^+ ratio in the

midlatitude NO^+/O_2^+
ble 5. Most of the
ng normal conditions.
ically between 2 and 5
969; Danilov, 1972).
e *E*-region during an
ailable, our own and
n give distinctly lower
vailable data strongly
tio in the *E*-region is
ng to the anomalous

the theoretical
al. (1970) (Fig. 14).

TABLE 5. DAYTIME NO^+/O_2^+ RATIOS IN THE *E*-REGION AT MIDDLE LATITUDES

	Altitude		
	110 km	120 km	130 km
Normal day			
Average of several rocket flights (see Monro and Bowhill, 1969; Danilov, 1972) ($\chi \approx 60°$)	3.	3	3
Anomalous day			
Our results (S-82) 14.12.71 ($\chi = 64°$)	.07	1.1	.98
Narcisi (1973) 31.1.69 ($\chi = 55.1°$)	1.2	1.2	1.2
Models			
Keneshea et al. (1970) ($\chi = 60°$)	1	.85	.8
Aikin and Goldberg (1973a) ($\chi = 53.2°$)	2.8	2.0	-
Hunt (1973) ($\chi = 60°$)	2.1	2.2	1.5

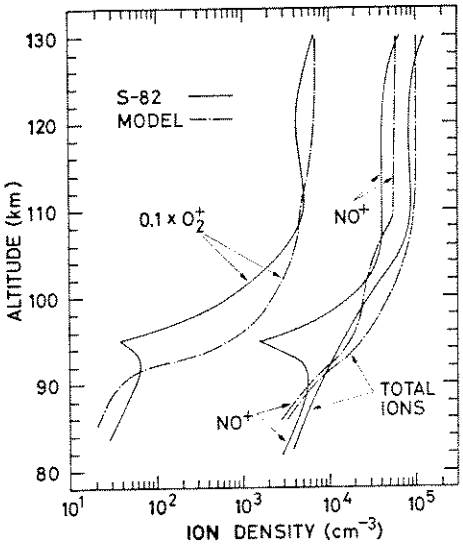

FIG. 14. COMPARISON OF OUR NO^+, O_2^+ AND TOTAL ION DENSITY PROFILES WITH THE CONCENTRATIONS PREDICTED BY KENESHEA *et al.* (1970).

Their model is essentially based on the NO measurements of Barth (1966), and, as noticed by Sechrist (1967), these measurements were performed during a winter day of high absorption. As seen in Fig. 14, the Keneshea *et al.* model gives a very good agreement with our measured NO^+, O_2^+ and electron concentration. The theoretical NO^+/O_2^+ ratios agree also very well with the values measured during anomalous conditions (see Table 5). Other models, based on 2 to 6 times higher NO concentrations above 95 km altitude, give NO^+/O_2^+ ratios between 1·5 and 3 in the 110–130 km region (Aikin and Goldberg, 1973a, Hunt, 1973; see Table 5).

All three models mentioned in Table 5 assume the same O density profiles (CIRA 1965). A change in the O concentration would, however, influence the NO^+/O_2^+ ratio in the *E*-layer in a similar manner as an NO variation. Thus, the depletion of NO and/or O in the *E*-region resulting from the postulated transport processes operating during anomalous winter days could easily explain the observed lowering of the NO^+/O_2^+ ratio.

From the foregoing discussion it seems evident that vertical transport was directly responsible for the observed increase in the mesospheric ion density. Enhanced transport will lead to an enhancement in the mesospheric concentrations of NO, O_3, O and H_2O (Shimazaki and Laird, 1970; Bowman *et al.*, 1970). An increase in NO and O_3 would increase the ion production by UV radiation ($NO + h\nu \rightarrow NO^+ + e^-$; $O_3 + h\nu \rightarrow O + O_2(^1\Delta g)$; $O_2(^1\Delta g) + h\nu \rightarrow O_2^+ + e^-$). The initially formed O_2^+ and NO^+ ions are intimately linked to the hydrated ions, as they represent the starting point of the water cluster production chains (cf. Thomas, 1972; Sechrist, 1972a). In this sequence of reactions an increase in the O/H_2O ratio will inhibit the formation of water cluster ions ($O_2^+O_2 + O \rightarrow O_2^+ + O_3$, Ferguson 1970, and probably $NO^+X + O \rightarrow NO_2^+ + X$ with $X = O_2$, N_2, CO_2 or H_2O, Swider 1972), thus reducing the electron loss. All these processes increase the electron density, and the problem is to ascertain the relative importance of each one in producing the winter anomaly (Geller and Sechrist, 1971).

From our measurements it is possible to calculate the NO density as well as the O_2^+ production rate. In the 80 km altitude interval NO^+ is the most abundant ion (see Fig. 12). The following equations should represent a good approximation to the NO^+ and O_2^+ production and losses in this altitude range (Thomas, 1972):

$$\begin{aligned} q(NO^+) &= \sigma\phi[NO] + k(O_2^+ - NO)[O_2^+][NO] \\ &\quad + k(O_2^+ - N_2)[O_2^+][N_2] \\ &= \alpha(NO^+)[NO^+][e^-] + \alpha(NO^+H_2O) \\ &\quad \times [NO^+H_2O][e^-] \\ &\quad + \beta\alpha(H^+(H_2O)_2)[H^+(H_2O)_2][e^-], \end{aligned} \tag{9}$$

$$\begin{aligned} q(O_2^+) &= \alpha(O_2^+)[O_2^+][e^-] + (1-\beta)\,\alpha(H^+(H_2O)_2) \\ &\quad \times [H^+(H_2O)_2][e^-] + \\ &\quad + k(O_2^+ - NO)[O_2^+][NO] \\ &\quad + k(O_2^+ - N_2)[O_2^+][N_2], \end{aligned} \tag{10}$$

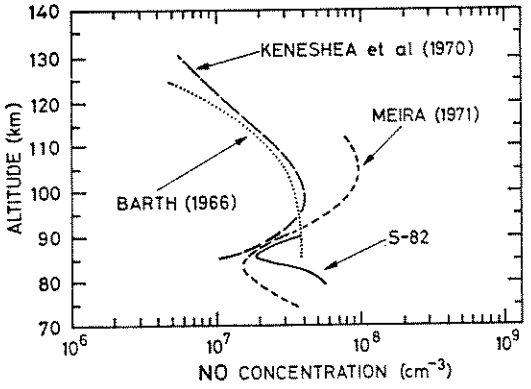

FIG. 15. COMPARISON OF NEUTRAL NO DENSITY DERIVED FROM S-82 DATA WITH DIRECT NO MEASUREMENTS (BARTH, 1966; MEIRA, 1971) AND THE PROFILE ADOPTED BY KENESHEA *et al.* (1970) IN THEIR MODEL.

The uncertainty in the rate constant $k(O_2^+ - N_2)$ introduces only an error of less than 10% in our NO density. The combination of the S-82 and the Keneshea *et al.* (1970) profiles should represent a fair approximation of the neutral NO density on an anomalous winter day.

with $\sigma = 2{\cdot}0 \times 10^{-18}$ cm^2 (Reid, 1970): effective ionization cross section of NO at the wave length of Lyman α. ϕ: flux of solar Lyman α radiation (Fig. 12 of Smith *et al.*, 1965; renormalized to $\phi_\infty = 3 \times 10^{11}$ photons cm^{-2} s^{-1} (Weeks, 1967)). $k(O_2^+ - N_2) \leq 3 \times 10^{17}$ cm^3 s^{-1} (Narcisi *et al.*, 1972): rate constant for $O_2^+ + N_2 \rightarrow NO^+ + NO$. $\alpha(NO^+H_2O) \approx 10^{-5}$ cm^3 s^{-1} (Goldberg and Aikin, 1971): rate constant for recombination of NO^+H_2O. $\alpha(H^+(H_2O)_2) = 3 \times 10^{-6}$ cm^3 s^{-1} (Biondi *et al.*, 1972): rate constant for recombination of $H^+(H_2O)_2$. β: fraction of $H^+(H_2O)_2$ produced through the NO^+ chain. For definitions and values of other constants see Section 7.

The equations assume that there is a fast link between NO^+ and NO^+H_2O. The effectiveness of the connection between NO^+H_2O and $H^+(H_2O)_2$ is not established (Niles *et al.*, 1972; cf. also Weill, 1973), and we therefore assume $0 \leq \beta \leq 1$. Losses by electron-ion recombination of the intermediate ions in both hydration sequences can be neglected.

Using Equation (9), the neutral NO number density can be calculated from the measured ion profiles (see Fig. 12). Below 83 km the measured 32^+ densities represent upper limits for the O_2^+ concentration as we cannot exclude the possible presence of S^+. Above 83 km S^+, if at all present, contributes less than 20% to the ion mass 32^+. The resulting uncertainty in the calculated NO density is less than 20%. The neutral NO densities thus derived from the S-82 ion profiles are shown in Fig. 15 together with the NO profiles measured by Barth (1966) and Meira (1971) and the profile used by Keneshea *et al.* (1970). The S-82 density of NO at lower altitudes is distinctly higher than the Meira profile. At approx. 90 km all profiles, except Barth (1966), give the same NO density within ±30%. The previous discussion of the NO^+/O_2^+ ratio in the *E*-region has shown that the Keneshea *et al.* (1970) model fits with the S-82 data in this altitude range. We may conclude that the combination of the S-82 and the Keneshea *et al.* profiles is a fair approximation of the neutral NO density in the 80–130 km range on an anomalous winter day.

Figure 16 shows the O_2^+ production rate profile calculated from the S-82 data using equation (10). For comparison, the expected production rate for a quiet day is given (Huffman *et al.*, 1971; Sechrist, 1972a). The O_2^+ production on 14 December 1971 is approximately an order of magnitude higher than the theoretical quiet day production. During the launch time, the 2–8 Å X-ray flux and the magnetic activity were fairly low (see Table 1), and an enhanced O_2^+ production by X-rays or particles seems

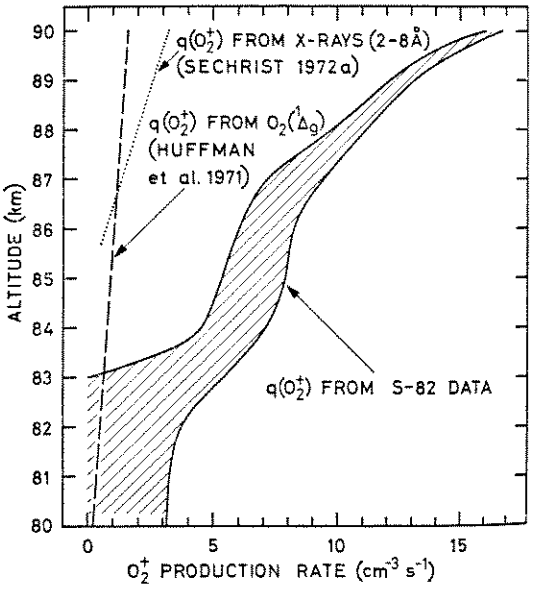

FIG. 16. COMPARISON OF O_2^+ PRODUCTION RATE DERIVED ACCORDING TO EQUATION (10) FROM THE S-82 DATA WITH THE THEORETICAL PRODUCTION FOR QUIESCENT CONDITIONS (HUFFMAN *et al.*, 1971; SECHRIST, 1972a).

The production from X-rays was adjusted to the flux actually observed during the flight (cf. Table 1). Below 83 km only an upper limit for $[O_2^+]$ and hence $q(O_2^+)$ can be given due to the possible presence of S^+. Furthermore, β is not known, and only an upper limit for $k(O_2^+ - N_2)$ is available (see text). These uncertainties are represented by the shaded region.

h the NO profiles measured
feira (1971) and the profile
l. (1970). The S-82 density
les is distinctly higher than
approx. 90 km all profiles,
e the same NO density within
discussion of the NO^+/O_2^+
is shown that the Keneshea
with the S-82 data in this
conclude that the combina-
Keneshea *et al.* profiles is a
e neutral NO density in the
anomalous winter day.

O_2^+ production rate profile
2 data using equation (10).
pected production rate for a
man *et al.*, 1971; Sechrist,
ction on 14 December 1971
er of magnitude higher than
y production. During the
X-ray flux and the magnetic
(see Table 1), and an en-
by X-rays or particles seems

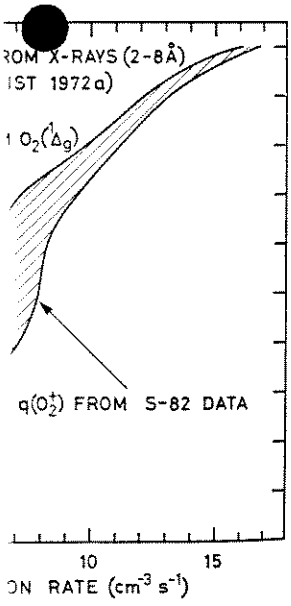

O_2^+ PRODUCTION RATE DERIVED
10) FROM THE S-82 DATA WITH
ION FOR QUIESCENT CONDITIONS
971; SECHRIST, 1972a).

ays was adjusted to the flux
he flight (cf. Table 1). Below
t for $[O_2^+]$ and hence $q(O_2^+)$
ssible presence of S^+. Further-
only an upper limit for
xt). These uncertainties
y the shaded region.

unlikely. The observed high $q(O_2^+)$ could be due to an increased O_3 concentration at these altitudes ($O_3 + h\nu \rightarrow O + O_2(^1\Delta g)$; $O_2(^1\Delta g) + h\nu \rightarrow O_2^+ + e^-$; see Hunt, 1973).

The observed enhanced vertical transport processes will also influence the concentration of other minor neutral constituents. As seen in Fig. 12, ion 50^+ ($O_2^+H_2O$) is detected at the level of maximum concentration of water cluster ions at 76 km, indicating that at this altitude the $O_2^+ \rightarrow$ hydrates sequence was proceeding and the O/H_2O ratio not significantly altered. Above 76 km—approx. 7 km lower than during quiescent conditions—the density of water cluster ions decreases abruptly, and NO^+ becomes dominant. This can be explained by an increased O/H_2O ratio due to the enhancement in vertical transport.

The ion 46^+ (NO_2^+) appears at 76 km and is most abundant at the altitude where NO^+H_2O has its maximum concentration. Under quiescent conditions at midlatitudes these ions are found only in the vicinity of 90 km, and their abundances are correlated (Aikin and Goldberg, 1973). The reaction $NO^+H_2O + O \rightarrow NO_2^+ + H_2O$ has been proposed in order to explain these measurements (Aikin and Goldberg 1973). Our observation of NO_2^+ at considerably lower altitudes is consistent with this process and reflects the increase of NO and /or O in the mesosphere. The disappearance of NO_2^+ above 77·5 km, where NO^+H_2O has still a relatively high concentration, indicates that the reaction $NO_2^+ + O \rightarrow NO^+ + O_2$ is the major loss process for NO_2^+ at the altitudes where atomic oxygen is abundant (Swider, 1972).

Our ion composition measurements in the *D*-region during the anomalous winter conditions can thus be explained in detail by the presence of increased vertical transport processes. In particular, enhancements of the NO density below 84 km, of the O_3 concentration between 80 and 90 km, and of the O/H_2O ratio above 76 km are required to explain our results.

Acknowledgements—We would like to thank Mr. H. Wyniger, H. Hofstetter, R. Liniger, J. Stettler, A. Juza, S. Schürch, L. André and F. Schweizer for their help during the design, building, and calibration phases of the mass spectrometer and associated electronics. We are grateful to Dr. E. Kopp and H. Balsiger and Mr. J. Fischer and L. Weber for their assistance and help at the launch site. We also wish to thank Drs. R. Jaeschke and A. Pedersen from ESTEC, Noordwijk, Holland, for making available to us their unpublished total electron and ion density measurements. We are indebted to Dr. W. Becker, Max Planck Institute, Lindau (F. R. G.), for the evaluation and comments on the ionograms, and to Dr. H. V. Widdel of the same institution for providing us with information on radio absorption. We thank Dr. J. O. Cardús from the Ebro Observatory, Tortosa, Spain, for providing us with information on magnetic conditions. We gratefully acknowledge Dr. R. Narcisi for kindly forwarding to us his unpublished results of the *E*-region on a winter anomalous day. One of us (M. A. H.) wishes to thank Drs. R. Narcisi and C. F. Sechrist, Jr., for their helpful discussions and criticisms, and is indebted to ESRO for a fellowship. Last, but not least, the careful typing of Mrs. M. Thönen, M. Schafroth and Miss E. Bühler is acknowledged.

Preparation and launching of the rocket was performed by ESRO. Our work was supported by the Swiss National Science Foundation (grants NF 5094, 2.73.68, 2.213.69, 2.405.70, 2.592.71, 2.768.72, 2.080.73 and 2.275.74).

REFERENCES

Aikin, A. C. and Goldberg, R. A. (1973a). Metallic ions in the equatorial ionosphere. *J. geophys. Res.* **78,** 734.

Aikin, A. C. and Goldberg, R. A. (1973b). Distribution of NO_2^+ in the lower ionosphere. *J. geophys. Res.* **78,** 1229.

Arnold, F. and Krankowsky, D. (1974). Measurements of $H_2O_2^+$ in the *D*-region and implications for mesospheric H_2O_2. *Geophys. Res. Lett.* **1,** 243.

Baldinger, E. and Nissen, H. (1967). Transformation automatique de la gamme de mesure pour des signaux très variables en amplitude. *Ber. Tag. Schweiz. Physik. Ges.* **18,** 923.

Balsiger, H., Eberhardt, P., Geiss, J. and Kopp, E. (1971). A mass spectrometer for the simultaneous measurement of the neutral and the ion composition of the upper atmosphere. *Rev. Sci. Instrum.* **42,** 475.

Barth, C. A. (1966). Rocket measurements of nitric oxide in the upper atmosphere. *Planet. Space Sci.* **14,** 623.

Belrose, J. S. and Thomas, L. (1968). Ionization changes in the middle latitude *D*-region associated with geomagnetic storms. *J. atmos. terr. Phys.* **30,** 1397.

Becker, W. (1972). Private communication.

Berkeljon, R., Englert, G., Jaeschke, R., Koehn, D., Pedersen, A., and Scheper, R. (1970). A rocket-borne, ejectable instrument package with parachute. Tech. Note ESRO TN-102 (ESTEC). Noordwijk, Holland.

Bibron, R., Chesselet, R., Crozaz, G., Leger, G., Mennessier, J. P. and Picciotto, E. (1974). Extraterrestrial ^{53}Mn in antarctic ice. *Earth Planet. Sci. Lett.* **21,** 109.

Biondi, M. A. (1969). Atmospheric electron–ion and ion–ion recombination processes. *Can. J. Chem.* **47,** 1711.

Biondi, M. A., Leu, M. T. and Johnsen, R. (1972). Recombination of electrons with positive ions of the $H_3O^+(H_2O)_n$ series. Aeron. Rept. 48. COSPAR Symp. on *D*- and *E*-region Ion Chemistry, p. 266. University of Illinois, Urbana, Illinois.

Black, D. C. (1972). On the origins of trapped helium, neon and argon isotopic variations in meteorites—II. Carbonaceous meteorites. *Geochim. Cosmochim. Acta* **36,** 377.

Bohachevsky, I. O. and Rubin, E. L. (1966). A direct method for computation of nonequilibrium flows with detached shock waves. *AIAA J.* **4,** 600.

Bowhill, S. A. (1969). Ion chemistry of the *D*- and *E*-regions. A survey for working group 11 of the

interunion commission on solar terrestrial physics. *J. atmos. terr. Phys.* **31,** 731.
Bowman, M. R., Thomas, L. and Geisler, J. E. (1970). The effect of diffusion processes on the hydrogen and oxygen constituents in the mesosphere and lower thermosphere. *J. atmos. terr. Phys.* **32,** 1661.
Burke, R. R. (1972). Comment on letter by W. Swider "Sources for $H^+(H_2O)_n$ ions in the *D*-region." *J. geophys. Res.* **77,** 1598.
Cardus, J. O. (1974). Private communication.
Cameron, A. G. W. (1968). A new table of the elements of the solar system. In *Origin and Distribution of the Elements* (Ed. L. H. Ahrens), p. 125. Pergamon Press, Oxford.
Chapman, S. (1956). The electrical conductivity of the ionosphere; a review. *Nuovo Cim.* **4,** 1385.
Chimonas, W. and Axford, I. (1968). Vertical movement of temperate-zone sporadic *E*-layers. *J. geophys. Res.* **73,** 111.
Christie, A. D. (1970). *D*-region winter anomaly and transport near the mesopause. *J. atmos. terr. Phys.* **32,** 35.
CIRA (1965). Cospar International Reference Atmosphere. North-Holland, Amsterdam.
Clayton, R. N., Grissmann, L. and Mayeda, T. K. (1973). A component of primitive nuclear composition in carbonaceous meteorites. *Science* **182,** 485.
Danilov, A. D. (1972). Ion composition and photochemistry of the *E*-region. Aeron. Rept. No. 48. COSPAR Symposium on *D*- and *E*-region ion chemistry (Ed. C. F. Sechrist, Jr. and M. A. Geller), p. 195. University of Illinois, Urbana, Illinois.
Dieminger, W., Rose, G., Schwentek, H., and Widdel, H. U. (1968). The morphology of winter anomaly of absorption. *Space Research VII* (Ed. R. L. Smith Rose), p. 228. North-Holland, Amsterdam.
Eberhardt, P. (1974). A neon *E*-rich phase in the Orgueil carbonaceous chondrite. *Earth Planet. Sci. Lett.* **26,** 182.
Fechtig, H. (1974). Private communication.
Fehsenfeld, F. C., Dunkin, D. B. and Ferguson, E. E. (1970). Rate constants for the reaction of CO_2^+ with O, O_2 and NO; N_2^+ with O and NO and O_2^+ with NO. *Planet. Space Sci.* **18,** 1267.
Ferguson, E. E. (1970). Laboratory measurements of *D*-region ion molecule reactions. In Mesospheric models and related experiments. *Proc. 4th ESRIN–ESLAB Symp.* Frascati, Italy, 6–10 July 1970, (Ed. G. Fiocco), p. 188. Reidel, Dordrecht, Holland.
Geisler, J. E. and Dickinson, R. E. (1968). Vertical motions and nitric oxide in the upper mesosphere. *J. atmos. terr. Phys.* **30,** 1505.
Geller, M. A. and Sechrist, G. F., Jr. (1971). Coordinated rocket measurements on the *D*-region winter anomaly—II. Some implications. *J. atmos. terr. Phys.* **33,** 1027.
Goldberg, R. A. and Blumle, L. J. (1970). Positive ion composition from a rocket borne mass spectrometer. *J. geophys. Res.* **73,** 133.
Goldberg, R. A. and Aikin, A. C. (1971). Studies of positive ion composition in the equatorial *D*-region ionosphere. *J. geophys. Res.* **76,** 8352.
Goldberg, R. A. and Aikin, A. C. (1972a). Comet Encke: Meteor metallic ion identification by mass spectrometer. Rept. X-625-72-402. Goddard Space Flight Center, Greenbelt, Maryland.
Gregory, J. B. and Manson, A. H. (1969). Seasonal variations of electron densities below 100 km at mid-latitudes—II. Electron densities and atmospheric circulation. *J. atmos. terr. Phys.* **32,** 837.
Hake, R. D., Jr., Arnold, D. E., Jackson, D. W., Evans, W. E., Ficklin, B. P. and Long, R. A. (1972). Dye-Laser observations of the nighttime atomic sodium layer. *J. geophys. Res.* **77,** 6839.
Hale, L. C. (1973). Positive ions in the mesosphere. Paper presented at Symp. B of the 16th Plenary Meeting COSPAR, 23 May, Konstanz, F. R. G.
Hines, C. O. (1972). Motions in the ionospheric *D*- and *E*-regions. *Phil. Trans. R. Soc. Lond.* (A) **271,** 457.
Hierl, P. M., Strattan, L. W. and Wyatt, J. R. (1973). A chemical accelerator for the study of the dynamics of ion–molecule reactions over the energy range 0·1–100 eV. *Int. J. Mass Spectrom. Ion Phys.* **10,** 385.
Howard, C. J., Rundle, H. W. and Kaufman, F. (1970). Gas phase reaction rates of some positive ions with water at 296°K. *J. chem. Phys.* **53,** 3745.
Huffman, R. E., Paulsen, D. E., Larrabee, J. C. and Cairns, R. B. (1971). Decrease in *D*-region $O_3(^1\Delta g)$ photoionization rates resulting from CO_2 absorption. *J. geophys. Res.* **76,** 1028.
Hughes, D. W. (1973). Interplanetary dust and its influx to the earth's surface. Paper presented at the Symp. B of the 16th Plenary Meeting COSPAR, 23 May, Konstanz, F. R. G.
Hunt, B. R. (1973). A generalized aeronomic model of the mesosphere and lower thermosphere including ionospheric processes. *J. atmos. terr. Phys.* **35,** 1755.
Istomin, V. G. and Pokhunkov, A. A. (1963). Mass spectrometer measurements of atmospheric composition in the USSR. *Space Res. III* (Ed. W. Priester), p. 117. North-Holland, Amsterdam.
Jaeschke, R. and Pedersen, A. (1972). Private communication.
Kato, S., Reddy, C. A. and Matsushita, S. (1968). Formation of sporadic *E*-layer due to wind shear in the presence of an electrostatic field. *Proc. 2nd Seminar on the Cause and Structure of Temperate Latitude Sporadic* E, p. V-4, September 1968, Vail, Colorado.
Keneshea, T. J., Narcisi, R. S. and Swider, W. (1970). Diurnal model of the *E*-region. *J. geophys. Res.* **75,** 845.
Krankowsky, D., Arnold, F., Wieder, H. and Kissel, J. (1972a). The elemental and isotopic abundance of metallic ions in the lower *E*-region as measured by a cryogenically pumped quadrupole mass spectrometer. *Int. J. Mass Spectrom. Ion Phys.* **8,** 379.
Lee, T. and Papanastassiou, D. A. (1974). Mg isotopic anomalies in the Allende meteorite and correlation with O and Sr effects. *Geophys. Res. Lett.* **1,** 225.
Lindblad, B., Arinder, G. and Wiesel, T. (1972). Continued rocket observations of micrometeorites. Paper presented at the 15th COSPAR Plenary Meeting, 10 May, Madrid, Spain.
Mahelum, B. (1967). On the winter anomaly in the mid-latitude *D*-region. *J. geophys. Res.* **72,** 2287.
Mechtly, E. A., Smith, L. G. and Henry, G. W. (1973). Rocket observations of the winter anomaly. Paper presented at the 16th COSPAR Plenary Meeting, 23 May, Konstanz, F. R. G.
Meira, L. G. (1971). Rocket measurements of upper atmospheric nitric oxide and their consequences to the lower ionosphere. *J. geophys. Res.* **76,** 202.

Millman, P. M. and McIntosh, B. A. (1964). Meteor radar statistics—I. *Can. J. Phys.* **42**, 1730.
Monro, P. E. and Bowhill, S. A. (1969). Minor atmospheric constituents and the ion composition of the *E*-region. *J. atmos. terr. Phys.* **31**, 103.
Narcisi, R. S. and Bailey, A. D. (1965). Mass spectrometric measurements of positive ions at altitudes from 64 to 112 km. *J. geophys. Res.* **70**, 3687.
Narcisi, R. S. (1968). Processes associated with metal–ion layers in the *E*-region of the ionosphere. *Space Research VIII* (Ed. A. P. Mitra, L. G. Jacchia, W. S. Newman), p. 360. North-Holland, Amsterdam.
Narcisi, R. S., Philbrick, C. R., Bailey, A. D. and Della Lucca, L. (1969). Review of daytime, sunrise and sunset ion composition of the *D*-region. Aeron. Rept. No. 32. Meteorological and chemical factors in *D*-region aeronomy—Record of the Third Aeronomy Conference (Ed. C. F. Sechrist, Jr.), p. 355. University of Illinois, Urbana, Illinois.
Narcisi, R. S. (1971). Composition study of the lower ionosphere. In *Physics of the Upper Atmosphere* (Ed. F. Verniani), p. 12. Casa Editrice Compositori, Bologna, Italy.
Narcisi, R. S. (1972). Mass spectrometer measurements in the ionosphere. In *Physics and Chemistry of Upper Atmospheres* (Ed. B. M. McCormac), p. 171. Reidel, Dordrecht, Holland.
Narcisi, R. S. Philbrick, C. R., Ulmick, J. C. and Gardner, M. E. (1972). Mesospheric nitric-oxide concentrations during a PCA. *J. geophys. Res.* **77**, 1322.
Narcisi, R. S. (1973). Private communication.
Niles, F. E., Heimerl, J. M. and Keller, G. E. (1972). Cluster, switch and rearrangement reactions for positive ions in the *D*-region. *Trans. Am. geophys. Union* **53**, 456.
Parker, L. W., Whipple, E. C. (1970). Theory of spacecraft sheath structure, potential and velocity effects on ion measurements by traps and mass spectrometers. *J. geophys. Res.* **75**, 4720.
Parthasarathy, R. and Rai, D. B. (1966). Effect of meteoric dust on the effective recombination coefficient in the lower ionosphere. *Radio Sci.* **1** (New Series), 1401.
Pedersen, A., Fahleson, U. and Faelthammar, C. G. (1972). Determination of the ionospheric density and temperature using a double probe electric field detector. *Space Research XII* (Eds. S. A. Bowhill, L. D. Jaffe and M. J. Rycroft), p. 1369. Akademie, Berlin.
Probstein, R. F. and Kemp, N. H. (1960). Viscous aerodynamic characteristics in hypersonic rarefied gas flow. *J. Aero. Space Sci.* **27**, 174.
Ratnasiri, P. A. J. (1972). Estimation of nitric oxyde concentration in the lower *E*-region from rocket and satellite measurements of electron densities and X-ray fluxes. Aeron. Rept. No. 48. COSPAR Symp. on *D*- and *E*-region Ion Chemistry (Eds. C. F. Sechrist, Jr. and M. A. Geller), p. 72. University of Illinois, Urbana, Illinois.
Reid, G. C. (1970). Production and loss of electrons in the quiet daytime *D*-region of the ionosphere. *J. geophys. Res.* **75**, 2551.
Rose, G., Weber, J., Widdel, H. U. and Galdon, P. (1973) Experimental results of radio wave absorption measurements in southwest Europe. Paper presented at the 16th Plenary Meeting COSPAR, 23 May, Konstanz, F. R. G.
Rutherford, J. A., Mathis, R. F., Turner, B. R. and Vroom, D. A. (1971). Formation of magnesium ions by charge transfer. *J. Chem. Phys.* **55**, 3785.
Rutherford, J. A., Mathis, R. F., Turner, B. R. and Vroom, D. A. (1972a). Formation of calcium ions by charge transfer. *J. Chem. Phys.* **57**, 3091.
Rutherford, J. A. and Vroom, D. A. (1972b). Formation of iron ions by charge transfer. *J. Chem. Phys.* **57**, 3091.
Sechrist, C. F., Jr. (1967). A theory of the winter absorption anomaly at middle latitudes. *J. atmos. terr. Phys.* **29**, 113.
Sechrist, C. F., Jr., Mechtly, E. A., Shirke, J. S. and Theon, J. S. (1969). Coordinated rocket measurements on the *D*-region winter anomaly—I. Experimental results. *J. atmos. terr. Phys.* **31**, 145.
Sechrist, C. F., Jr. (1972a). Theoretical models of the *D*-region. *J. atmos. terr. Phys.* **34**, 1565.
Sechrist, C. F., Jr. (1972b). Interactions between the neutral atmosphere and the lower ionosphere. In *Thermospheric Circulation* (Ed. W. L. Webb), p. 261. MIT Press, Cambridge, Mass.
Shahin, M. M. (1966). Mass spectrometric studies of corona discharges in air at atmospheric pressures. *J. Chem. Phys.* **45**, 2600.
Shimazaki, T. and Laird, A. R. (1970). A model calculation of the diurnal variation in minor neutral constituents in the mesosphere and lower thermosphere including transport effects. *J. geophys. Res.* **75**, 3221.
Smith, L. G., Accardo, C. A., Weeks, L. H. and McKimeon, P. J. (1965). Measurements in the ionosphere during the solar eclipse of 20 July 1963. *J. atmos. terr. Phys.* **27**, 803.
Swider, W., Jr. (1969). Processes for meteoric elements in the *E*-region. *Planet. Space Sci.* **17**, 1233.
Swider, W. (1970). Sources for $H_3O^+ \cdot (H_2O)_n$ ions in the *D*-region. *J. geophys. Res.* **75**, 7299.
Swider, W. (1972). Reply to a comment on a letter by W. Swider: "Sources for $H^+ \cdot (H_2O)_n$ ions in the *D*-region". *J. geophys. Res.* **77**, 1998.
Thomas, L. (1968). The electron density distribution in the *D*- and *E*-regions during days of anomalous radio wave absorption in winter. *J. atmos. terr. Phys.* **30**, 1211.
Thomas, L. (1971). The lower ionosphere. *J. atmos. terr. Phys.* **33**, 157.
Thomas, L. (1972). *D*- and *E*-region aeronomy. Aeron. Rept. No. 48. COSPAR Symposium on *D*- and *E*-region ion chemistry (Eds. C. F. Sechrist, Jr. and M. A. Geller), p. 1. University of Illinois, Urbana, Illinois.
Thorness, R. B. and Nier, A. O. (1962). Device for remote opening of a vacuum system. *Rev. Sci. Instrum.* **33**, 1005.
Urey, M. C. (1964). A review of atomic abundances in chondrites and the origin of meteorites. *Rev. Geophys.* **2**, 1.
Weeks, L. U. (1967). Lyman-alpha emission from the sun near solar minimum. *Astrophys. Lett.* **3**, 1203.
Weill, G. (1973). Summary of the summer advanced study institute, Orleans. In *Physics and Chemistry of Upper Atmospheres* (Ed. B. M. McCormac), p. 357. Reidel, Dordrecht, Holland.
Widdel, H. U. (1973). Private communication.

Zbinden, P. A. (1971). Ein Massenspektrometer mit Cryopumpe zur Messung der positiven Ionen in der unteren Ionosphäre. Ph.D. Thesis, University of Bern, Bern, Switzerland.

Zbinden, P. A., Hidalgo, M. A., Eberhardt, P. and Geiss, J. (1974). Positive ion composition in the lower ionosphere during the Geminid meteor shower and the occurrence of a winter anomaly. *Space Research XIV* (Ed. K. Rawer), p. 19. Akademie, Berlin.

Zimmerman, S. P. and Narcisi, R. S. (1970). The winter anomaly and related transport phenomena. *J. atmos. terr. Phys.* **32**, 1305.